Journal of Plankton Research, 2025, **47**, fbaf034
https://doi.org/10.1093/plankt/fbaf034
Original Article

Planktonic associations in the Northern Bering and Chukchi seas during the 2017–2019 warm period

Silvana Gonzalez[1,*], Jens M. Nielsen[2,3], Lisa B. Eisner[2], David G. Kimmel[2], Michael W. Lomas[4], Russell Hopcroft[5], Miranda Hart[6], Elizabeth Logerwell[2], Astrid Schnetzer[6], Adam Spear[2] and James T. Thorson[2]

[1]Institute of Marine Research, Oceanography and Climate, Strandgaten 196, Bergen 5004, Norway
[2]NOAA, Alaska Fisheries Science Center, 7600 Sand Point Way NE, Seattle, WA 98115, USA
[3]Cooperative Institute for Climate, Ocean, and Ecosystem Studies, University of Washington, 3737 Brooklyn Ave NE, Seattle, WA 98105, USA
[4]Bigelow Laboratory for Ocean Sciences, Phytoplankton Ecology and Biogeochemistry Laboratory, 60 Bigelow Dr., East Boothbay, ME 04544, USA
[5]College of Fisheries and Ocean Sciences, University of Alaska, 2150 Koyukuk Drive, Fairbanks, AK 99775, United States
[6]Department of Marine, Earth and Atmospheric Sciences, North Carolina State University, 2800 Faucette Dr, Raleigh, NC 27607, USA

*Corresponding author: silvana.gonzalez@hi.no

Corresponding editor: Marja Koski

ABSTRACT

Pacific Arctic ecosystems are changing due to ocean warming and sea ice loss. Increases in primary production and shifts towards smaller phytoplankton and zooplankton have been recently documented, yet understanding interactions among plankton components and their responses to changing oceanographic conditions are still needed. Herein, we assess plankton responses to unprecedented warm water temperatures and low sea ice conditions during springs and summers of 2017–2019 in the Northern Bering and Chukchi seas. Record low sea ice in winter 2017–2018 was followed by high biomass of large phytoplankton (>5 μm) but low abundances of large mesozooplankton (>500 μm) species in spring of 2018, potentially due to a temporal mismatch between zooplankton and phytoplankton. The widespread distribution of warm Coastal Water in the Chukchi Sea during summer of 2019 resulted in increased biomass of small-sized phytoplankton and a mesozooplankton community characterized by small copepod species and neritic copepods. Planktonic food webs changed seasonally, with phytoplankton and mesozooplankton directly linked in spring but mediated by microzooplankton in summer. Shifts towards smaller plankton with warming will increase the number of trophic levels and reduce trophic transfer efficiencies with potential impacts on fish and shellfish resources and benthic-pelagic coupling in these ecosystems.

KEYWORDS: Chukchi Sea; Northern Bering sea; phytoplankton; zooplankton; planktonic food web

INTRODUCTION

Arctic and subarctic regions, including the Northern Bering and Chukchi seas, are undergoing rapid changes as a result of ocean warming (Stroeve and Notz, 2018; Danielson *et al.*, 2020; Timmermans and Labe, 2020). Increasing ocean temperatures over the last century are coupled with drastic reductions in sea ice extent, thickness, and duration (Markus *et al.*, 2009; Serreze *et al.*, 2016; Kwok, 2018; Wu and Wang, 2018) that affect underwater light fields, nutrient availability in the water column and bloom dynamics (Mundy *et al.*, 2005; Arrigo *et al.*, 2014; Hill *et al.*, 2018). From 2014 to 2021 unprecedented high water temperatures and low winter and spring sea ice cover (Stabeno *et al.*, 2019; Danielson *et al.*, 2020; Ballinger and Overland, 2022) were recorded in the Northern Bering and Chukchi seas, with 2017–2021 being documented as a period of remarkable ecosystem change (Huntington *et al.*, 2020; Siddon *et al.*, 2020; Baker *et al.*, 2020b; Ballinger and Overland, 2022).

Changes in oceanographic conditions have a direct and rapid impact on planktonic communities in the Pacific Arctic (Questel *et al.*, 2013). Warming and sea ice loss have been associated with changes in the magnitude of annual primary production (Lewis *et al.*, 2020; Kwon *et al.*, 2022), changes in the timing of the spring bloom (Hirawake *et al.*, 2021; Song *et al.*, 2021), northward expansion of boreal species distributions (i.e. borealization) (Mueter *et al.*, 2021; Axler *et al.*, 2023), and shifts in phytoplankton and zooplankton size and species composition (Li *et al.*, 2009; Ershova *et al.*, 2015b). Warming and changes in nutrient availability and form can shift size spectra to smaller phytoplankton and zooplankton through decreased individual sizes and/or replacement of large species by smaller species (Daufresne *et al.*, 2009; Gardner *et al.*, 2011; Mueter *et al.*, 2021). Smaller phytoplankton species have been associated with warmer temperatures in the Canadian Basin (Li *et al.*, 2009), the broader North Atlantic (Morán *et al.*, 2010), Chukchi Sea (Fujiwara *et al.*, 2014;

Received: August 28, 2024. **Revised:** March 19, 2025. **Accepted:** June 2, 2025

Fujiwara and Cohen, 2015) and in experiments using Arctic species (Coello-Camba *et al.*, 2015). Similar shifts from large-bodied, ice-associated, and typically lipid-rich zooplankton to smaller and often less nutritious zooplankton species have been observed in the Northern Bering and Chukchi seas (Ershova *et al.*, 2015b; Kimmel *et al.*, 2023) and other Arctic regions (Aarflot *et al.*, 2018; Møller and Nielsen, 2019).

Shifts in species and size composition of planktonic communities affect trophic interactions, energy pathways, and benthic-pelagic coupling, potentially altering the entire structure of Arctic marine ecosystems and the services they provide to human communities (Mueter *et al.*, 2021). Changes in planktonic species composition affect the quality of food available for upper trophic levels (Heintz *et al.*, 2013) as nutritional composition and edibility vary among species even within the same size class (Galloway and Winder, 2015; Jónasdóttir, 2019). Shifts towards smaller phytoplankton and zooplankton increases the number of trophic levels and reduces trophic transfer efficiency in marine ecosystems, which results in less energy available for upper-trophic-level species including fish, seabirds and marine mammals (Barnes *et al.*, 2010; Carozza *et al.*, 2019; Mueter *et al.*, 2021). A potential shift to smaller primary producers also highlights the increasing role that microzooplankton, primarily ciliates and dinoflagellates, may play in mediating carbon transfer to mesozooplankton (Campbell *et al.*, 2009; Stoecker *et al.*, 2017). The complex array of feeding behaviors associated with these grazer populations presents unique challenges in constraining carbon transfer at the inter, and intraprotistan level (Caron *et al.*, 2012; García-Oliva *et al.*, 2022). For instance, while some dinoflagellates may feed on microplankton of similar size (Hansen *et al.*, 1994, 1997), others may also be significant grazers on nano- and pico-sized prey (Fulfer and Menden-Deuer, 2021; García-Oliva *et al.*, 2022). These shifts in planktonic food webs are also expected to reduce the amount of ungrazed phytoplankton that reaches the seafloor, leading to major reductions in benthic biomass and weakening benthic-pelagic coupling characteristic of this region (Grebmeier, 2012; Lovvorn *et al.*, 2016; Waga *et al.*, 2019).

In this study, we examine how different oceanographic conditions during a period of extreme warming impacted the plankton community across multiple trophic levels in the Northern Bering and Chukchi seas. Specifically, we looked at shifts in phytoplankton, microzooplankton, and mesozooplankton spatial distributions, taxonomic composition, and size structure in association with oceanographic conditions using data from four Arctic Integrated Ecosystem Research Program (Arctic IERP) surveys conducted in springs of 2017 and 2018 and summers of 2017 and 2019. We also looked at the causal relationships among plankton components using structural equation models (SEM) to understand how seasonal and interannual variations in oceanographic conditions may affect trophic interactions and food web trophic efficiency. We hypothesized that warm conditions would favor smaller phytoplankton and zooplankton species affecting the structure of the planktonic food web (i.e. changes in the strength and sign of correlations). Our comprehensive study of planktonic responses during these recent extreme warm conditions provides insight into how plankton and Arctic marine ecosystems may respond to continued increase in mean water temperatures.

METHODS

Study area

The Northern Bering and Chukchi seas consist of extensive, shallow (average < 70 m), and biologically productive continental shelves greatly influenced by seasonal sea ice cover and northward-flowing Pacific water masses (Walsh, 1989; Springer *et al.*, 1996). For much of the year (October–May), the region remains ice covered with a cold well-mixed water column (Hunt *et al.*, 2013). When sea ice starts to melt after May, a stratified, warmer, nutrient-rich water column supports large phytoplankton blooms (Arrigo *et al.*, 2012) that in some regions can continue into the summer until nutrient exhaustion (Hill *et al.*, 2018). These large phytoplankton blooms combined with relatively low pelagic grazing and shallow bathymetry result in a large amount of pelagic production being exported to the bottom supporting large benthic biomass (Grebmeier *et al.*, 2015) and aggregations of benthic-feeding marine mammals in the area (Jay *et al.*, 2012). In autumn, the intensification of winds and diminishing solar input allows the water column to re-homogenize and surface waters are replenished with nutrients that support open water phytoplankton blooms until sunlight fades (Waga and Hirawake, 2020).

The region is dominated by northward currents that transport heat, salt, nutrients, and plankton from the North Pacific into the Arctic (Hunt *et al.*, 2016) through the Bering Strait (Fig. 1). This transport is driven by a seasonally fluctuating Pacific–Arctic pressure head (Stigebrandt, 1984; Aagaard *et al.*, 2006) that transmits 1.0–1.2 Sv of water during summer and 0.5–0.6 Sv of water during winter months (Woodgate *et al.*, 2005). Water flowing through the Bering Strait is routed across the Chukchi shelf along three main pathways: Herald Canyon in the west, Barrow Canyon in the east and the Central Channel across the mid-shelf (Fig. 1), other factors, primarily wind, can episodically modify or even reverse these flows (Weingartner *et al.*, 2005; Woodgate *et al.*, 2005; Danielson *et al.*, 2014). A strong density front typically separates the Alaskan Coastal Water from offshore Bering Shelf and Anadyr Waters, and from colder Arctic-origin waters farther north (Gawarkiewicz *et al.*, 1994; Weingartner *et al.*, 2005).

Data collection and processing

Four surveys were conducted in the Northern Bering and Chukchi Sea region as part of the Arctic IERP (Baker *et al.*, 2020a; Baker *et al.*, 2023) during spring of 2017 and 2018, and late summer/early autumn of 2017 and 2019. Spring Arctic Shelf Growth, Advection, Respiration, and Deposition Rate Experiments (ASGARD) surveys were conducted on 9–28 June in 2017 and on 4–25 June in 2018 on the RV *Sikuliaq* covering the Northern Bering and Southern Chukchi seas. Summer Arctic Integrated Ecosystem Surveys (IES) were conducted during 1 August–28 September in 2017 and 1 August–3 October in 2019 on the RV *Ocean Starr* in the Eastern Chukchi Sea (see Fig. 2 for sampling locations for each cruise). Data used in our analyses are publicly available in the DataONE repository (https://arctic-ierp.dataportal.nprb.org/).

Vertical profiles of temperature and salinity were collected at each station using a Sea-Bird Electronics (SBE) 911+ CTD

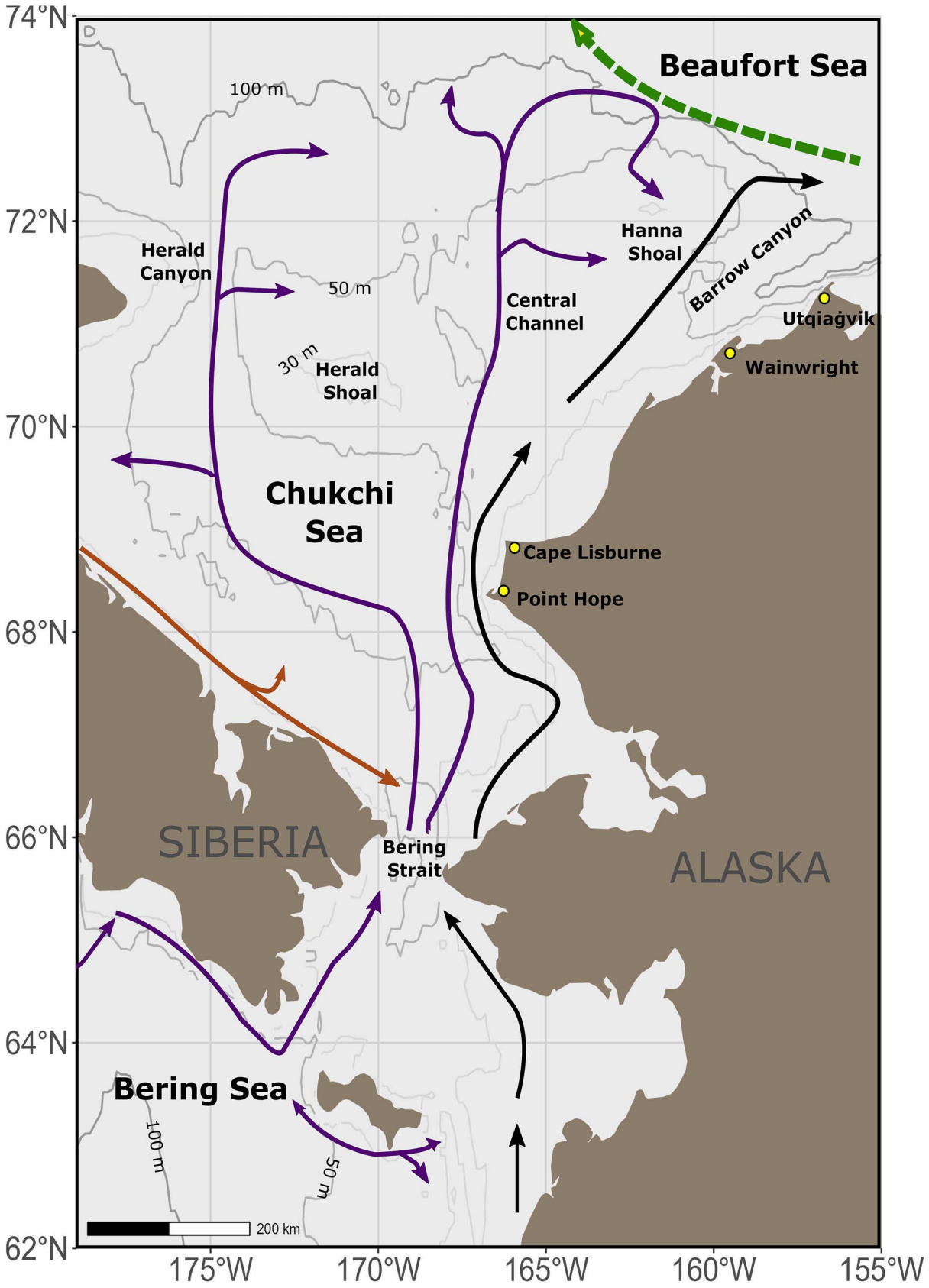

Fig. 1. Study region map with main flow pathways. A thick green dashed arrow represents the Beaufort Gyre, a black arrow along the US coast represent the Alaskan Coastal Current, a brown arrow along the Siberian coast represents the Siberian Coastal Current, and mid-positioned purple arrows represent pathways of the Bering shelf, Anadyr, and Chukchi shelf currents. Contour lines indicate 30 m, 50 m, and 100 m isobaths. Modified from (Danielson *et al.*, 2020).

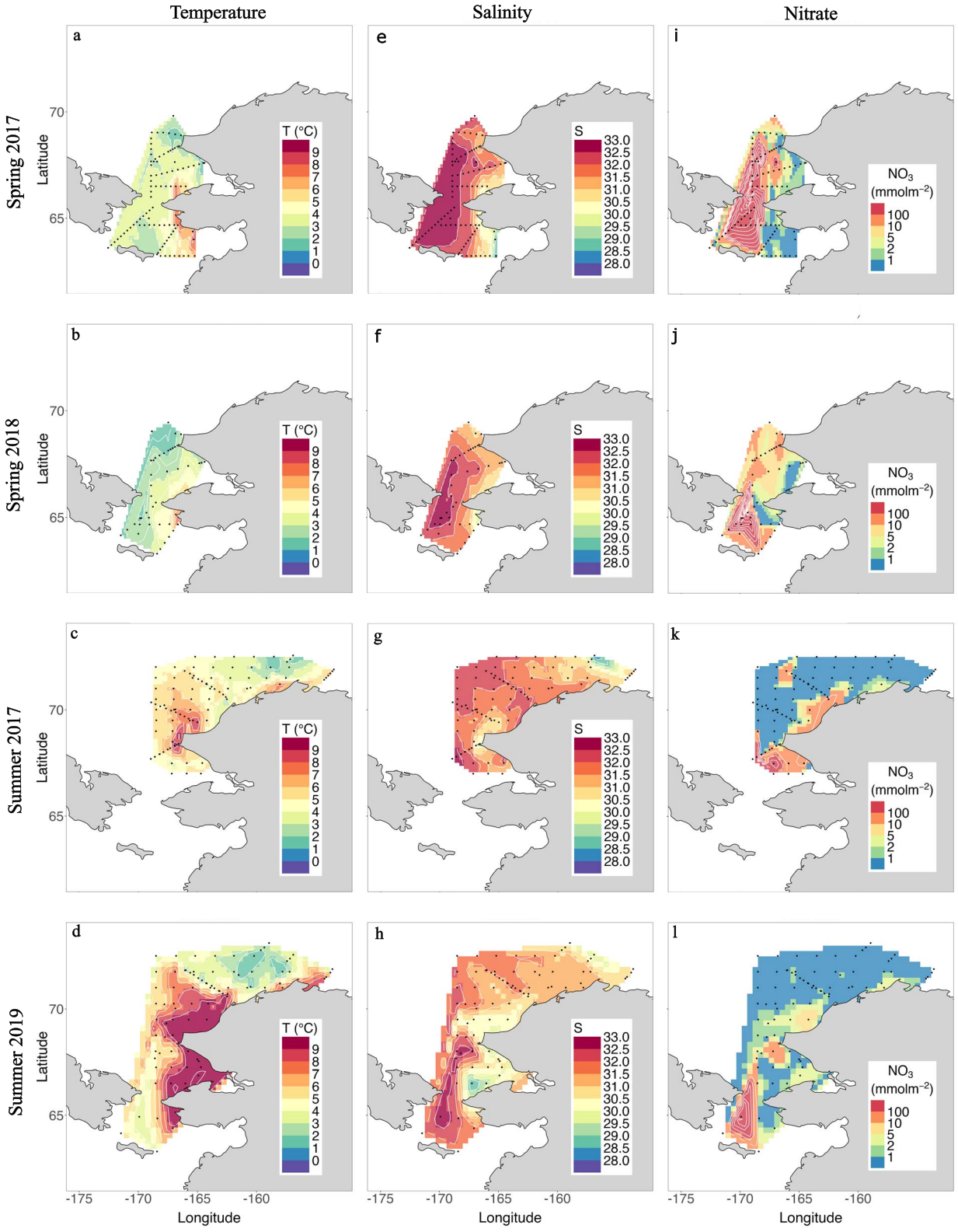

Fig. 2. Interpolated values of sea water temperature (**a**–**d**) and salinity (**e**–**h**) averaged for top 50 m of the water column, and integrated surface (i.e. above mixed layer depth) nitrate concentration (**i**–**l**) observed during the four Arctic IERP surveys conducted in springs of 2017 and 2018 (ASGARD) and summers of 2017 and 2019 (IES) in the Northern Bering Sea and Chukchi Sea. Black points indicate sampled stations.

averaged into 1 m bins. The depth of the pycnocline (mixed layer depth), defined as the first depth at which density was 0.10 kg m^{-3} greater than the density at a depth of 5 m (Danielson *et al.*, 2011), and a stratification index (SI) that indicates the density difference between the top and bottom 5 m of the water column, were calculated using the R package *castr* version 0.1.0 (Irisson, 2024). Temperature and salinity were averaged for the full water column (or top 50 m), and above and below the mixed layer depth. Water masses were assigned to each 1 m depth layer based on temperature and salinity characteristics following the Danielson *et al.* (2020) classification. The most frequent water mass, above and below the mixed layer depth, was selected as the predominant surface and bottom water mass at each station.

Water samples were collected from 5 L (IES 2017), 10 L (IES 2019) or 12 L (ASGARD, 2017–2018) Niskin bottles attached to a CTD rosette. At every sampling station, total and size-fractioned (<5, 5–20, > 20 μm or <5 and >5 μm, depending on survey/station) chlorophyll *a* (Chl*a*; mg m^{-3}) samples were collected. Total Chl*a* samples were commonly collected at 10 m intervals (~5–6 depths) and filtered through 25 mm Whatman GF/F filters (nominal pore size 0.7 μm). Size-fractionated samples were collected at 2–3 depths using a stacked filtration unit, using 47 mm Whatman GF/F filters (or 25 mm GF/F when sampling two size fractions) for < 5 μm, and 47 mm polycarbonate filters with a pore size of 5 and 20 μm, to sample the 5–20 and >20 μm size fractions. Filters were stored frozen (−80°C) and analyzed within 6 months with a calibrated bench top Turner Designs Trilogy fluorometer using standard extraction methods (Parsons, 1984).

Samples for dissolved inorganic nutrients (nitrate, nitrite, ammonium, phosphate and silicic acid; μmol kg^{-1}) were collected from each sample depth, filtered through 0.45 μm cellulose acetate filters, and frozen. Samples were analyzed on a Seal AA3 or Seal AA500 continuous segmented flow analyzer following methods in (Gordon *et al.*, 1993). Ammonium was analyzed using the fluorescent o-phthalaldehyde (OPA) method (Holmes *et al.*, 1999). To increase vertical resolution of Chl*a* measurements, *in vivo* fluorescence data profiles were calibrated with discrete Chl*a* samples by fluorometer and year. Calibrated Chl*a* profiles were obtained by regressing discrete Chl*a* samples against fluorometer measurements at the same depths. Depth profiles of size-fractionated Chl*a* were estimated by linearly interpolating the proportion of each Chl*a* size fraction from discrete samples (>5 μm/total Chl*a*, 5–20 μm/total Chl*a*, > 20 μm/total Chl*a*) and multiplying the total integrated Chl*a* from calibrated *in vivo* fluorometer data by each size fraction proportion. We calculated Chl*a* in the > 5 μm size fraction by combining Chl*a* in the 5–20 μm and >20 μm size fractions.

For the characterization of microplankton assemblages, seawater was collected at the surface (0–10 m), at the deep/subsurface Chl*a* maximum (DCM), and at an additional depth between the DCM and the bottom. In the absence of a DCM feature, a second depth was sampled mid-way between surface depth and the bottom. Samples for characterizing microplankton assemblages via microscopy (100 ml) were immediately preserved with Acid Lugol's solution (5% final concentration). Microplankton enumeration and identification were completed by inverted light microscopy (200x) using standard settling techniques (Utermöhl, 1958). Microplankton were assigned to three taxonomic groups (ciliates, dinoflagellates and diatoms) based on morphological examination (Tomas, 1997; Boltovskoy, 1999). Microplankton genera were also categorized based on their functional modes as phototrophs (diatoms), heterotrophs (tintinnids and specific dinoflagellate genera), and mixotrophs (Mitra *et al.*, 2023). Cell biovolume (BV) was calculated from geometric shapes (i.e. cylindrical, spherical, ellipsoidal, conical) of at least nine individual organisms, typically three representatives for each of the three most common genera within each major protist group. Average BVs were converted into carbon (C) biomass by applying published conversion factors for ciliates with 0.19 pg C μm^{-3}, and for diatoms and dinoflagellates with pg C μm^{-3} = 0.288 $BV^{0.811}$ and pg C μm^{-3} = 0.76 $BV^{0.819}$, respectively (Menden-Deuer and Lessard, 2000). Nutrient concentration, total and size-fractionated Chl*a* concentrations, and microplankton biomass were integrated throughout the entire water column for stations < 50 m depth, or the top 50 m for station depths >50 m.

Zooplankton were collected using vertical hauls of twin-ring nets (60 cm mouth, 150 μm mesh) and oblique bongo tows (60 cm frame, 505 μm mesh) in ASGARD surveys or oblique tows of paired bongo nets (20 cm frame, 153 μm mesh and 60 cm frame, 505 μm mesh, Napp *et al.*, 1996; Incze *et al.*, 1997) in IES surveys. A comparison of zooplankton abundance estimates from the two smaller mesh-size gears (oblique and vertical) deployed at the same locations during two surveys in the Chukchi Sea showed that the data from these two gears are comparable (see Kimmel *et al.*, 2023 supplemental material). The tows were within 5–10 m of the bottom depending on sea state, and depth was monitored continuously using a SeaBird FastCAT 49 CTD. Volume filtered was estimated using a General Oceanics flowmeter mounted inside the mouth of each net. Samples were preserved in 5% buffered formalin/seawater. Zooplankton were identified to the lowest taxonomic level and stage possible either at the University of Alaska Fairbanks (ASGARD) or at the Plankton Sorting and Identification Center in Szczecin, Poland, and verified at the Alaska Fisheries Science Center, Seattle, Washington, USA (IES). Only taxa contributing > 1% to total abundance (Table I) were included in statistical analyses. Abundance of mesozooplankton (ind. m^{-3}) was converted to biomass (mg C m^{-3}) using literature values (Supplementary Material 1) for its use in the SEM analysis section.

Statistical analysis

Interannual differences in oceanographic conditions and plankton components

We used Student's t-test statistic and Kruskal–Wallis test ($P < 0.05$) for detection of significant interannual differences in mean oceanographic and biological variables within each season (Table II). Water column temperature and salinity, and surface nutrient concentration values were linearly interpolated for the spatial domain of each cruise using the R package *akima* version 0.6 (Akima and Gebhardt, 2022). Interannual and seasonal variations in spatial patterns of mesozooplankton communities were assessed using Hierarchical Cluster Analysis (HCA) based on the Bray–Curtis similarity matrix. We applied a fourth-root

Table I: *List of taxonomic groups included in statistical analyses, gear (mesh size in μm), abbreviation, and zooplankton stage or size limit.*

Taxa	Gear	Abbreviation	Stage
Acartia spp.∗	150	AC	C1–C6
Bivalvia	150	BI	Larvae
Centropages spp.	150	CP	C1–C6
Cirripedia	150	CI	Nauplius/Cypris
Echinodermata small	150	ECS	Larvae
Fritillaria spp.	150	FR	<20 mm
Oikopleura spp. small	150	OK.S	<20 mm
Oithona spp.∗	150	OI	C1–C6
Polychaeta small	150	PS	Larvae
Pseudocalanus spp.∗	150	PC	C1–C6
Calanus glacialis∗∗	150/505	CG	C1–C6
Epilabidocera longipedata	150/505	EL	C1–C6
Eucalanus bungii∗∗	150/505	EB	C1–C6
Euphausiacea	150/505	EU	Calyptopis, Furcilia, Juvenile, Adult
Metridia spp.	150/505	ME	C1–C6
Neocalanus spp.∗∗	150/505	NE	C1–C6
Tortanus discaudatus	150/505	TD	C1–C6
Aglantha digitale	505	AD	Medusa
Brachyura	505	BR	Larvae
Calanus hyperboreus∗∗	505	CAH	C3–C6
Chaetognatha	505	CH	<20 mm
Echinodermata large	505	ECL	Larvae
Limacina helicina	505	LH	<20 mm
Oikopleura spp. large	505	OK.L	<20 mm
Paguridae	505	PA	<20 mm
Polychaeta large	505	PL	Larvae
Thysanoessa spp.	505	TH	<20 mm

Mesh size labeled as 150 corresponds to mesh sizes of 150 μm or 153 μm. Asterisks indicate copepod species included in structural equation models: ∗ indicates small copepods and ∗∗ indicates large copepods.

transformation to the zooplankton abundance data to reduce the effect of rare species, and calculated the Bray–Curtis similarity index (Bray and Curtis, 1957) using the R package *vegan* version 2.6.4 (Oksanen *et al.*, 2022). The HCA was implemented using the R package *cluster* version 2.1.4 (Oksanen *et al.*, 2022). We performed an indicator species analysis (Dufrêne and Legendre, 1997) using the R package *indicspecies* version 1.7.12 (De Cáceres and Legendre, 2009) to examine which taxa were indicative of each group from the HCA. The indicator species analysis produces an indicator species value (*IndVal*) that ranges from 0 to 1. Taxa that are selected as indicators of a group are those with *IndVal* closest to 1 where an *IndVal* of 1 indicates taxa are found within their group only. Permutation tests ($n = 999$) were carried out to determine the significance of taxa as indicators at $\alpha = 0.05$ (i.e. significant indicators were those identified in 95% of permutation replicates).

Environmental drivers of mesozooplankton community composition

We used redundancy analyses (RDAs, Bocard *et al.*, 2011) to examine relationships between the mesozooplankton community and environmental variables using the *vegan* R package (Oksanen *et al.*, 2022). We conducted an RDA using data from all cruises combined and from spring and summer cruises separately to assess differences in zooplankton abundance and environmental associations between and within seasons. Before RDA, we used Spearman correlation to remove environmental variables that were highly correlated with others ($P > 0.5$) to prevent overestimation of the explained variation. Latitude, longitude, bottom depth, mixed layer depth, sea surface temperature and salinity, water-column integrated Chl*a* concentrations in the > 5 μm and < 5 μm size fractions, and water-column integrated ciliate and dinoflagellate biomass were all included in RDAs as environmental predictors. Environmental variables were natural log-transformed and all variables were standardized into 0–1 ranges prior to analysis. A stepwise model selection approach, adding/removing variables at each step until no change was identified, was performed to identify significant explanatory variables (number of permutations = 10 000) for each RDA. We used the variation inflation factor to test for any remaining collinearity in each model.

Effects of temperature on plankton components and their associations

SEM were used to quantify hypothesized causal relationships among planktonic components and sea temperature and compare these relationships across seasons and years. SEM are probabilistic models that connect multiple predictor and response variables in a single causal network, thereby allowing simultaneous tests of multiple hypotheses and quantification of both direct and indirect or cascading effects (Grace and Keeley, 2006; Grace *et al.*, 2010; Lefcheck, 2016). SEM are often represented using path diagrams where arrows indicate hypothesized directional relationships between observed variables that are then captured in a set of structured equations. The strength of the relationships between variables is given as unstandardized and

Table II: *Mean, standard deviation (SD), and median of studied variables during Arctic IERP spring (ASGARD) and summer (IES) surveys including mean water column, surface, and bottom temperature and salinity, integrated surface nutrient concentrations, water column integrated total and size fractionated chlorophyll a (Chla) concentrations, water column integrated ciliates, dinoflagellates and total microzooplankton biomass, and mean abundances of large and small copepod species (see Table I).*

	Spring 2017 ($n = 53$)		Spring 2018 ($n = 32$)		Summer 2017 ($n = 67$)		Summer 2019 ($n = 58$)	
Variable	**Mean ± SD**	**Median**	**Mean ± SD**	**Median**	**Mean ± SD**	**Median**	**Mean ± SD**	**Median**
Temperature (°C)	3.62 ± 1.48∗	3.40	2.93 ± 1.28∗	2.69	4.75 ± 1.61∗	4.87	5.89 ± 2.85∗	5.26
Surface temperature (°C)	5.08 ± 2.23	4.77	4.29 ± 1.64	3.81	5.43 ± 1.10∗	5.60	7.98 ± 1.95∗	8.54
Bottom temperature (°C)	2.83 ± 1.58∗	2.76	1.89 ± 1.35∗	1.81	3.48 ± 1.62∗	3.46	4.82 ± 3.47∗	3.95
Salinity	32.00 ± 0.94	32.2	31.90 ± 0.75	32.00	31.5 ± 0.77∗	31.60	31.10 ± 0.86∗	31.20
Surface salinity	31.60 ± 1.24	32.0	31.3 ± 1.02	31.4	31.0 ± 1.36∗	31.4	29.9 ± 1.19∗	29.9
Bottom salinity	32.1 ± 0.86	32.3	32.2 ± 0.67	32.3	32.1 ± 0.45∗	32.2	31.6 ± 0.82∗	31.8
Nitrate (mmol m^{-2})	155 ± 275	2.46	48.3 ± 104	9.55	10.5 ± 34.5∗	0.00	2.04 ± 7.54∗	0.00
Nitrite (mmol m^{-2})	2.15 ± 3.45	0.22	0.96 ± 1.57	0.37	0.56 ± 1.13∗	0.18	0.27 ± 0.56∗	0.05
Ammonium (mmol m^{-2})	28.2 ± 46.3	6.71	11.4 ± 13.7	6.78	11.7 ± 27.2∗	2.75	5.03 ± 10.2∗	0.49
Phosphate (mmol m^{-2})	20.7 ± 26.0	6.53	16.1 ± 13.1	10.50	12.0 ± 7.88∗	11.5	7.33 ± 4.40∗	5.94
Silicate (mmol m^{-2})	271 ± 445	41.0	102 ± 150	57.2	83.9 ± 120∗	38.6	68.1 ± 59.4∗	45.6
Total Chl*a* (mg m^{-2})	96.2 ± 113	65.5	128 ± 105	102.0	53.6 ± 26.3	50.2	52.9 ± 21.7	47.8
Chl*a* < 5 μm (mg m^{-2})	23.7 ± 19.5∗	17.6	10.4 ± 5.38∗	9.3	14.2 ± 9.34∗	12.2	22.8 ± 15.7∗	19.6
Chl*a* > 5 μm (mg m^{-2})	97.4 ± 154	44.1	125 ± 109	104.0	41.6 ± 23.0∗	37.2	29.6 ± 17.2∗	26.8
Diatoms (mg C m^{-2})	327.0 ± 1017∗	23.7	608.0 ± 1295∗	210	321.0 ± 668	74.2	100.0 ± 92.7	55.4
Total microzooplankton (mg C m^{-2})	644.0 ± 1103∗	186.0	591 ± 553∗	375	999.0 ± 808∗	731	496.0 ± 385∗	451
Ciliates (mg Cm^{-2})	423.0 ± 731	146.0	164.0 ± 101	158.0	417.0 ± 350∗	281	183 ± 236.0∗	47.3
Dinoflagellates (mg C m^{-2})	221.0 ± 397∗	66.9	427.0 ± 509∗	223.0	582 ± 601	283	313 ± 226	284
Large copepods (ind. m^{-3})	204.0 ± 324∗	155.0	30.1 ± 24.8∗	21.0	20.7 ± 63.2	0.49	8.40 ± 13.3	3.11
Small copepods (ind. m^{-3})	5 626 ± 7 069	3 717	5 079 ± 3 804	4 318	3 644 ± 4708∗	1 457	6 119 ± 4957∗	4 409

∗ Indicates significant differences in variables mean values between years within a season.

standardized (in units of standard deviations) regression coefficients. Unstandardized regression coefficients are used to compare the strength of the same relationships across models (i.e. across model comparison) and standardized regression coefficients are used to compare the relative strength of the different relationships within a model (i.e. within model comparisons). The variables included in the model were mean water temperature, integrated Chl*a* concentrations in the < 5 μm size fraction and in the > 5 μm size fraction (includes Chl*a* from large phytoplankton cells and mixotrophic microzooplankton), heterotrophic microzooplankton biomass, and small and large copepod biomass. "Small copepods" included copepod species caught in the 150 μm net as adults (i.e. early stages of large copepods were not included in this group): *Acartia* spp., *Pseudocalanus* spp., and *Oithona* spp. "Large copepods" included stages CIII-Adult of *Calanus hyperboreus*, and stages CIV-Adult of the species *Calanus glacialis*, *Eucalanus bungii*, and *Neocalanus* spp. (Table I). The variables included in the model were selected in a way that maximizes the number of distinct trophic levels and size classes while maintaining a good model fit. We chose biomass over abundance to better represent the trophic structure of the community. The overall goodness of fit for SEM was assessed via a χ^2-test, and the standardized root mean square residual (SRMR). A good model fit is indicated by a non-significant χ^2-test (i.e. P-value > 0.05) and low (< 0.08) SRMR. SEM were conducted using the R package *lavaan* version 0.6.12 (Rosseel, 2012).

All statistical analyses were performed using R version 4.2.2.

RESULTS

Oceanographic conditions

During the warm period of 2017–2019, we observed interannual variability in oceanographic conditions (Figs 2 and 3, Table II). In spring, water column and bottom temperatures in the Northern Bering and southern Chukchi seas were higher in 2017 compared to 2018 (Fig. 2a and b, Table II). In 2018, bottom water masses in the region were predominantly composed of nutrient-rich Anadyr (AnW) and cool Shelf Water (cSW) whereas in 2017, warm Shelf Water (wSW) occupied a larger portion of the region (Fig. 3b). In spring, surface (i.e. above mixed layer depth) nutrient concentrations (nitrate, nitrite, ammonium, silicate and phosphate) were consistently high (> 1 mmol m^{-2}) throughout most of the region (see Fig. 2i and j for nitrate and Fig. S1 of Supplementary Material 2 for the other nutrients).

In summer of 2019, the Chukchi Sea was warmer (Fig. 2c and d) and less saline (Fig. 2g and h) compared to 2017 (Table II). These differences were more accentuated in surface waters, where mean temperature and salinity differences exceeded 2°C and 1, respectively, between 2017 and 2019 (Table II). In summer of 2019, the Chukchi Sea shelf was mainly occupied by warm Coastal Water (wCW) with wSW, the predominant water mass in 2017, restricted to areas farther from shore (Fig. 3). Summer surface nitrate concentrations in the Chukchi Sea were higher in 2017 compared to 2019 (Table II). The prevalence of less saline surface waters in 2019, particularly in nearshore areas of the Chukchi Sea, resulted

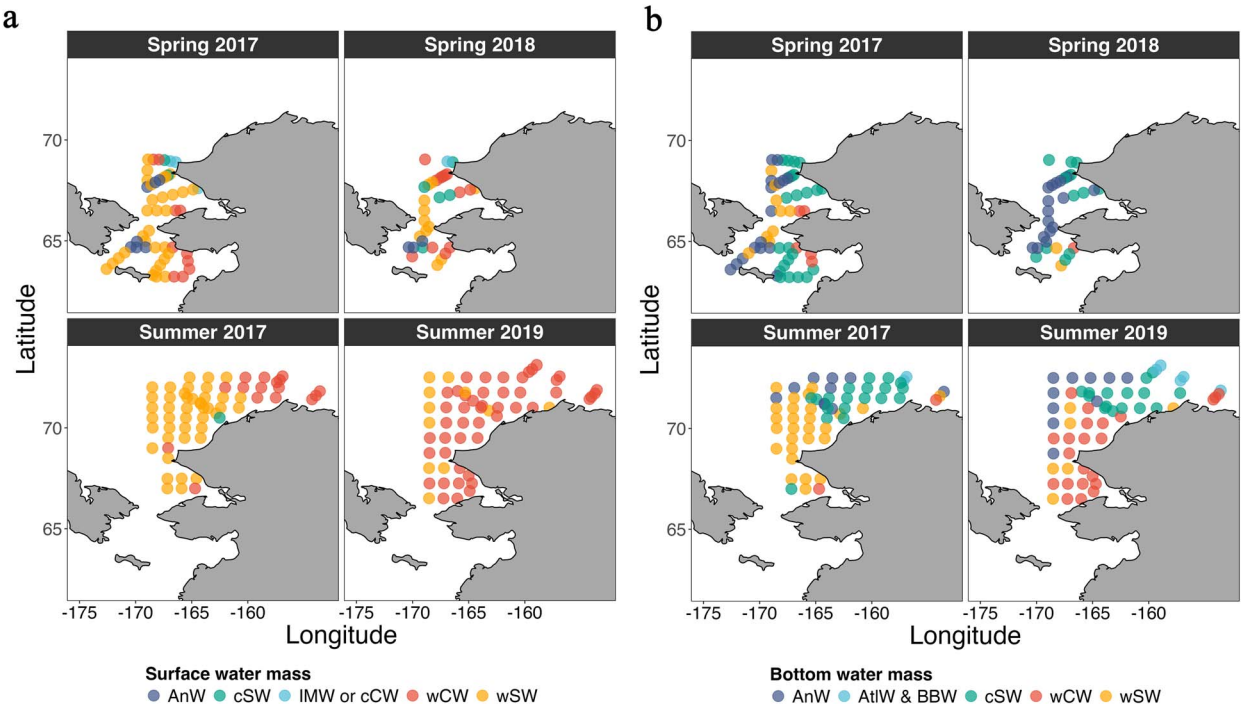

Fig. 3. Predominant surface (**a**) and bottom (**b**) water masses in springs of 2017 and 2018 (ASGARD) and summers of 2017 and 2019 (IES). AnW, Anadyr Water; cSW, cool Shelf Water; IMW, Ice Melt Water; cCW, cool Coastal Water; wCW, warm Coastal Water; wSW, warm Shelf Water; AtlW, Atlantic Water; BBW, Bering Basin Water.

in shallow mixed layer depths and strong stratification (Fig. S2 of Supplementary Material 2) that were associated with low nitrate concentrations (<1 mmol m^{-2}) in the surface mixed layer throughout most of the Chukchi Sea shelf (Fig. 2k and l).

Phytoplankton and microzooplankton distributions

Seasonal and interannual variability in oceanographic conditions was associated with variations in phytoplankton and microzooplankton biomass and distribution (Fig. 4). Water column integrated total Chl*a* was, averaged over all stations, significantly higher in spring ($P < 0.05$; median = 73.8 mg m^{-2}, interquartile range (IQR) = 35.2–139.0 mg m^{-2}) than in summer (median = 47.8 mg m^{-2}, IQR = 37.9–65.6 mg m^{-2}), although high variability existed among stations and surveys (Table II, Fig. 4a–d). In spring, when nutrient concentrations were highest and large phytoplankton is typically dominant, we observed a significantly lower predominance of Chl*a* in the < 5 μm size fraction (mean contribution = 23%) compared to summer (mean contribution = 37%) (*P*-value < 0.05, Fig. 4e–h). Total microzooplankton biomass was significantly higher (*P*-value < 0.05) in summer (median = 503 mg C m^{-2}) than spring (median = 335 mg C m^{-2}).

In spring of 2018, the spring with earlier sea ice retreat and relatively cooler water temperatures, we observed almost two times higher diatom biomass compared to spring of 2017 (Fig. 4a and b, Table II). Total integrated microzooplankton biomass was lower in spring of 2018 compared to 2017 with dinoflagellates being the predominant group in 2018 and ciliates in 2017 (Table II).

In summer, averages of integrated total Chl*a* were similar in 2017 and 2019 (Table II). However, warmer summer conditions in 2019 were characterized by a greater predominance of Chl*a* in the < 5 μm size fraction ($mean_{2017}$ = 28%; $mean_{2019}$ = 44%), mainly in areas with wCW (Figs 3 and 4g and h). Ciliate biomass was lower in 2019 compared to 2017 (Table II), particularly in areas with wCW, resulting in a lower total microzooplankton biomass in 2019 ($median_{2017}$ = 731 mg C m^{-2}, $median_{2019}$ = 451 mg C m^{-2}) (Fig. 4i–l).

Mesozooplankton

The abundances of small and large copepods (see Table I) were significantly (*P*-value < 0.05) higher in spring ($median_{small}$ = 4 138 ind. m^{-3}, $median_{large}$ = 76.2 ind. m^{-3}) than summer ($median_{small}$ = 3 354 ind. m^{-3}, $median_{large}$ = 1.55 ind. m^{-3}). In spring of 2018, the year with earlier sea ice retreat, we observed lower abundances of large copepods on average compared to spring of 2017 (Table II). In summer, the mean abundance of small copepods was two times higher in 2019, the warmest year, compared to that of 2017 (Table II). Zooplankton taxonomic composition for each survey can be found in Fig. S3 and Table S1 of Supplementary Material 2.

Based on cluster analysis of zooplankton community composition (taxa shown in Table I), four groups of stations were identified and the distribution of these groups varied across surveys (Fig. 5, and Fig. S4 and Table S2 of Supplementary Material 2). Group 1 (76 stations) was represented by samples collected in the spring in the Northern Bering Sea and southern portion of the Chukchi Sea (Fig. 5) and was particularly characterized by the occurrence of *Neocalanus* spp. (*IndVal* = 0.93)

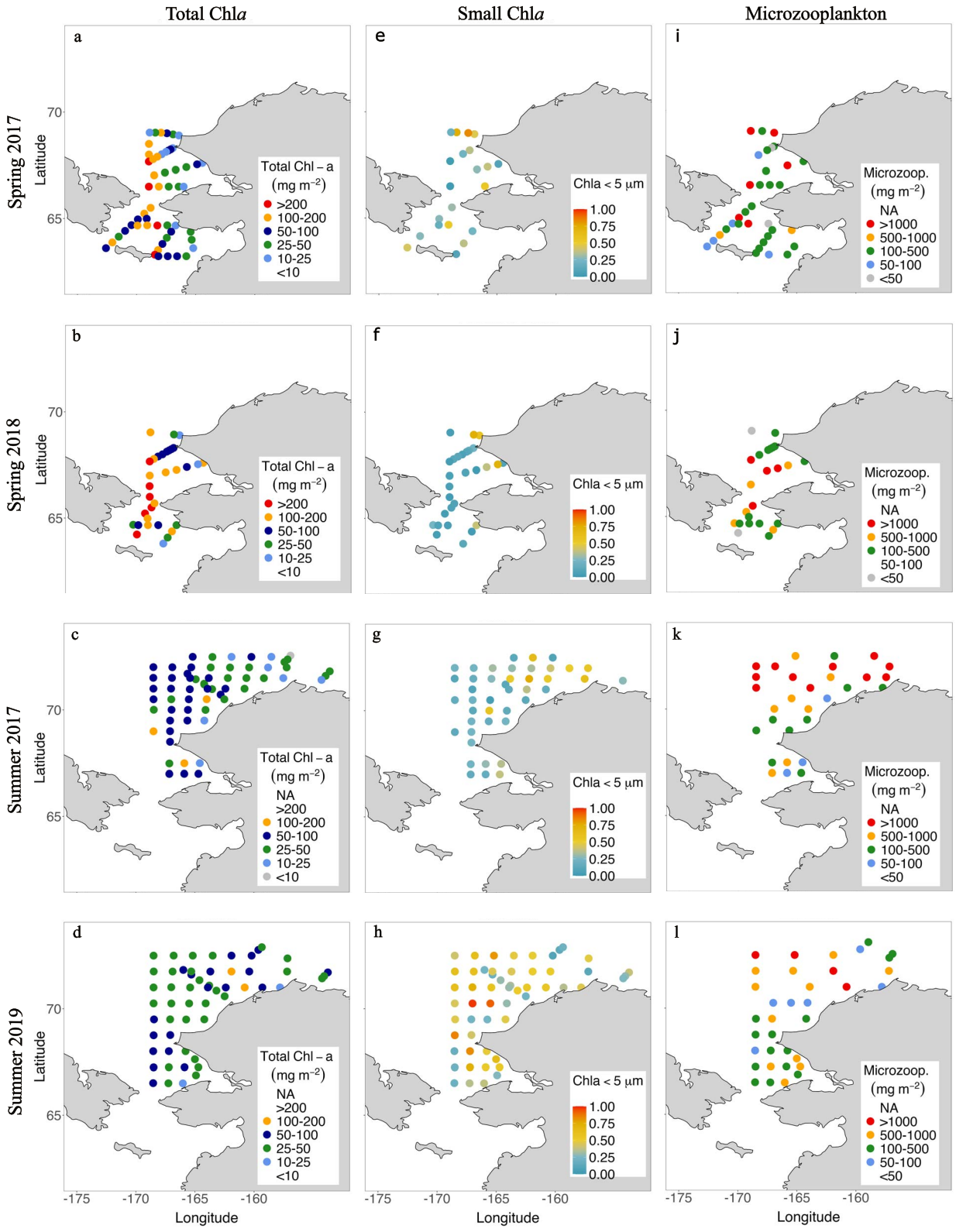

Fig. 4. Integrated water column total Chl*a* (**a**–**d**), proportion of integrated < 5 μm Chl*a* size fraction (<5 μm Chl*a*/total Chl*a*) (**e**–h), and integrated total microzooplankton (ciliates + dinoflagellates) biomass (**i**–**l**) observed during the four Arctic IERP surveys conducted in spring of 2017 and 2018 (ASGARD) and summers of 2017 and 2019 (IES) in the Northern Bering Sea and Chukchi Sea.

copepods of Pacific origin. Group 2 (67 stations) distribution was centered in the northern Chukchi Sea in summer and was defined by the combined occurrence of the large, cold water copepods *C. glacialis* and *C. hyperboreus* (*IndVal* = 0.52). Group 3 (42 stations) showed a nearshore distribution both in spring and summer and was characterized by the occurrence of the neritic copepods *Epilabidocera longipedata* and *Tortanus discaudatus* (*IndVal* = 0.82). In 2017, this group was mainly restricted to nearshore waters of the southern portion of the Chukchi Sea. In contrast, in 2019 this cluster occupied a broader area of the Chukchi Sea shelf, reaching higher latitudes and offshore waters following the distribution of warm Coastal Water (Figs 3 and 5). Group 4 (25 stations) was located in the central portion of the Chukchi Sea in summer and was characterized by the occurrence of small echinoderms (*IndVal* = 0.77). Group 4 distribution was wider in summer of 2017 when warm Coastal Water was restricted to nearshore locations and warm Shelf Water was the predominant water mass over the shelf (Figs 3 and 5c and 5d). Notably, in areas where spring and summer sampling overlapped (between the Bering Strait and Cape Lisburne for 2017), stations clustered differently by season with all spring sampling locations classified as group 1 while groups 2 to 4 were present in summer. This reinforces the idea that seasonal changes in environmental conditions, rather than spatial location alone, drive zooplankton community structure.

Environmental drivers of mesozooplankton distribution

The combined RDA, including all cruise data, showed distinct seasonal/regional associations between environmental variables and zooplankton taxa abundances (Fig. 6a–c). The best model fit (adjusted $r^2 = 0.37$) identified by stepwise selection included location, sea surface temperature, bottom depth, surface salinity, Chl*a* <5 μm, ciliate biomass, and mixed layer depth as the variables correlated with zooplankton community composition (see Table S3 in Supplementary Material 2). Zooplankton composition varied seasonally (Fig. 6a–c). Spring samples were characterized by high abundances of copepods *C. glacialis*, *Metridia* spp., *Neocalanus* spp., *Pseudocalanus* spp., and of other zooplankton including Paguridae decapods, euphausiids, polychaetes and the mollusk *Limacina helicina* (Fig. 6b and c). These taxa were positively associated with salinity and negatively associated with water temperature (Fig. 6a–c). Summer samples were characterized by high abundances of the neritic copepods *T. discaudatus* and *E. longipedata*, the small copepods *Oithona* spp. and *Acartia* spp., bivalve larvae, and the tunicates *Oikopleura* spp. (Fig. 6b and c). These taxa were positively associated with sea surface temperature and the < 5 μm Chl*a* size fraction and negatively correlated with surface salinity (Fig. 6b and c). Some species abundant in summer samples such as *C. hyperboreus*, small echinoderm larvae, and the appendicularia *Fritillaria* spp. were less associated with seasonal differences in measured environmental conditions. Instead, their occurrences were more directly linked to the geographic location of the collected samples (Fig. 6a–c). In particular, *C. hyperboreus* is an Arctic species found mainly at the northern end of the sampling area and thus does not experience the full range of environmental conditions across the study region. This limited distribution likely explains its stronger association with geography rather than with environmental variables. The strong separation between spring and summer samples in both zooplankton groups and environmental variables suggest that while spatial variations may interact with seasonal differences, seasonality is likely the dominant structuring factor.

RDAs focused on within season variations in zooplankton composition showed interannual differences in zooplankton community and associated environmental variables (Fig. 6d–i). Spring best fit model (adjusted $r^2 = 0.21$) included surface salinity, longitude, and Chl*a* < 5 μm (Fig. 6d–f and Table S3 in Supplementary Material 2). Spring 2018 samples were characterized by low concentrations of Chl*a* <5 μm and greater abundances of small mesozooplankton including *Centropages* spp., *Acartia* spp., *T. discaudatus, Pseudocalanus* spp. and small echinoderms and polychaetes (Fig. 6d–f). In summer, the best fit model (adjusted $r^2 = 0.24$) included latitude, longitude, sea surface temperature, and bottom depth (Fig. 6g–i and Table S3 in Supplementary Material 2). Summer 2019 stations were associated with increasing sea surface temperatures and higher abundances of the neritic copepods *T. discaudatus*, *E. longipedata*, the small copepod *Oithona* spp., and bivalves (Fig. 6g–i, Fig. S3, and Table S3 of Supplementary Material 2).

Planktonic associations

SEM (χ^2-test *P*-value = 0.08, and SRMR = 0.07) showed that relationships among plankton components were highly variable across surveys (Fig. 7, Table S4 of Supplementary Material 2). The effects of mean water column temperature on large copepod biomass were negative in both summer surveys and not significant in spring. The effect of temperature on small copepod biomass was positive in summer of 2017 and 2019, and not significant in spring surveys. Overall, we observed a greater number of significant links among planktonic communities in summer than in spring. In spring, Chl*a* >5 μm had a significant direct effect on copepod and heterotrophic microzooplankton biomass, while no significant effects of microzooplankton on copepod biomass were observed (Fig. 7a). However, in summer, there were no direct effects of Chl*a* (<5 μm or >5 μm) on copepod biomass, instead, Chl*a* effects on copepods were only indirect, fully mediated by microzooplankton (Fig. 7b). The effect of temperature on Chl*a* >5 μm was positive in summer of 2017 and negative during summer of 2019 when warmer and fresher conditions were associated with lower nutrient concentrations in the region.

DISCUSSION

Characterization of planktonic communities during spring

High diatom biomass in spring of 2018 relative to that of 2017, was likely associated with differences in the timing of sea ice retreat between the 2 years. In the Northern Bering Sea, interannual differences in phytoplankton size composition are associated with timing of sea ice retreat and nutrient availability (Fujiwara *et al.*, 2016). In 2017, the spring phytoplankton bloom occurred in early May (Nielsen *et al.*, 2024) and was tightly synchronized with sea ice retreat that year (Kikuchi *et al.*, 2020). However, in 2018, sea ice retreat occurred earlier (mid-April)

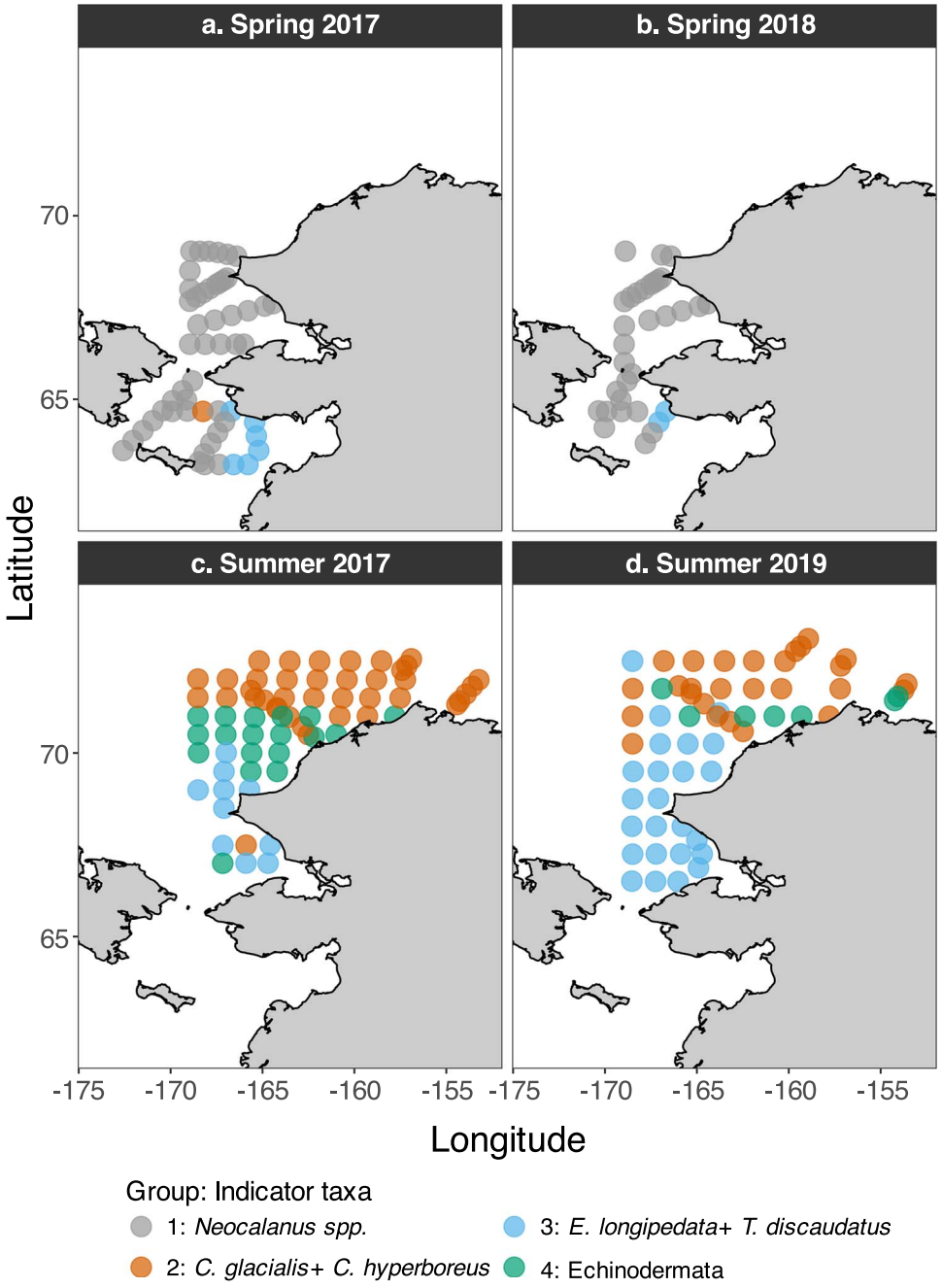

Fig. 5. Horizontal distribution of the four groups identified from the Bray–Curtis similarity index based on zooplankton abundance data in the Northern Bering Sea and Chukchi Sea during springs of 2017 and 2018 (ASGARD) and summers of 2017 and 2019 (IES). Indicator taxa, identified using an indicator species analysis, are shown for each group.

and during a time of strong winds that prevented water column stratification. These conditions prevented an ice-edge bloom and resulted in a delayed open water spring bloom in late May of 2018 (Kikuchi *et al.*, 2020; Nielsen *et al.*, 2024). The timing of our surveys could also explain some of the differences in large phytoplankton between the two springs, with our 2018 survey conducted closer to the time of the bloom compared to 2017. Our observations of higher phytoplankton biomass in 2018 relative to that of 2017 and under extreme low sea ice conditions are consistent with Park *et al.* (2021). These authors observed relatively high phytoplankton biomass compared to a 2003–2020 average for the Northern Bering and Southern Chukchi seas in association with the exceptionally early and broad open water extent that spring. These observations imply that increased open water extent, and consequently, increased light availability, promoted phytoplankton growth, and increased open ocean primary production that spring.

Low sea ice, early sea ice retreat and delayed spring bloom in 2018 in the Bering Sea were associated with shifts in zooplankton species composition. The community structure of mesozooplankton is affected not only by water mass characteristics but also by the timing of the phytoplankton bloom (Kimura *et al.*,

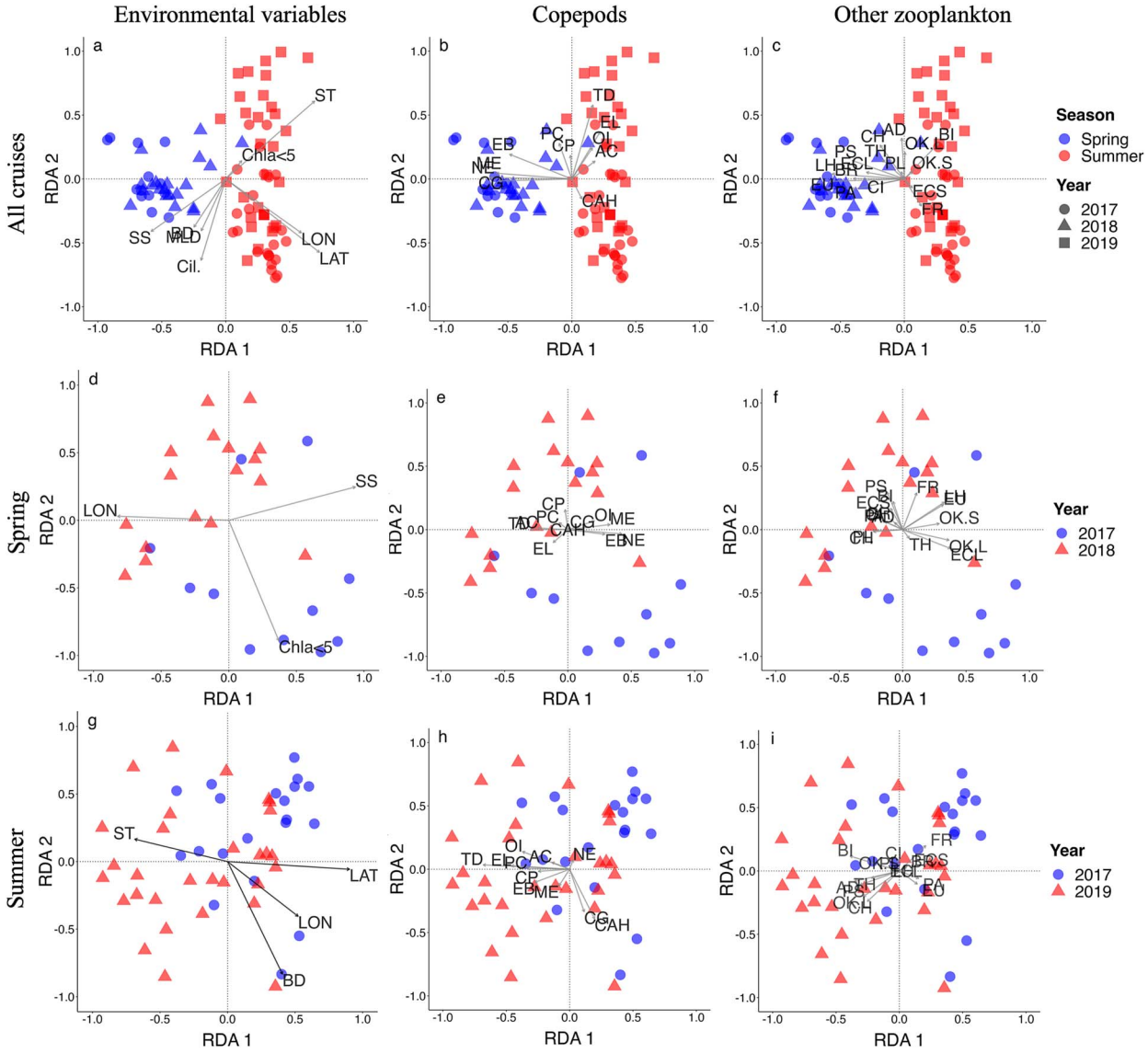

Fig. 6. Redundancy analysis biplots showing environmental variables (**a**, **d**, **g**), copepod species (**b**, **e**, **h**), and other zooplankton taxa (**c**, **f**, **i**) including all (a–c), spring (d–f), and summer (g–i) cruises. Each data point represents a station. ST, sea surface temperature (°C); SS, sea surface salinity; BD, bottom depth (m); LON, longitude; LAT, latitude; Cil., water column integrated ciliate biomass (mg C m^{-2}); MLD, mixed layer depth (m); Chl*a* <5, water column integrated chlorophyll *a* <5 μm size fraction (mg m^{-2}). Zooplankton taxa abbreviations are found in Table I.

2020). More specifically, many copepod species including *C. glacialis* have synchronized their seasonal migration, reproduction, and growth with the primary production regime in Arctic shelf seas (Søreide *et al.*, 2010). Our observations agree with Kimura *et al.* (2022) who observed that in 2018 the zooplankton community was dominated by small copepods and younger stages of large copepods (*C. glacialis* and *Metridia pacifica*), likely caused by reproduction delays resulting from the early sea-ice retreat and a delayed phytoplankton bloom that year. Early sea ice retreat and delayed phytoplankton bloom, in combination with relatively lower water temperatures recorded in spring of 2018 may have contributed to increased developmental times and reduced growth, resulting in the relatively low abundances of large copepods observed in our study. Relatively higher water temperatures recorded during spring of 2017 were associated with a greater predominance of ciliates and higher abundances of larger copepods (e.g. *Neocalanus* spp., *E. bungii*). The predominance of ciliates in spring of 2017 may be associated with earlier availability of phytoplankton (earlier phytoplankton bloom associated with sea ice retreat in 2017) and warmer temperatures closer to that for ciliates maximum growth [~5°C; (Franzè and Lavrentyev, 2014)]. Similarly, greater abundances of large copepods in spring of 2017 compared to 2018 was likely related to higher temperatures driving increases in growth rate and egg production, and reductions in development times (Hirst & Bunker, 2003) in synchrony with a timely phytoplankton bloom.

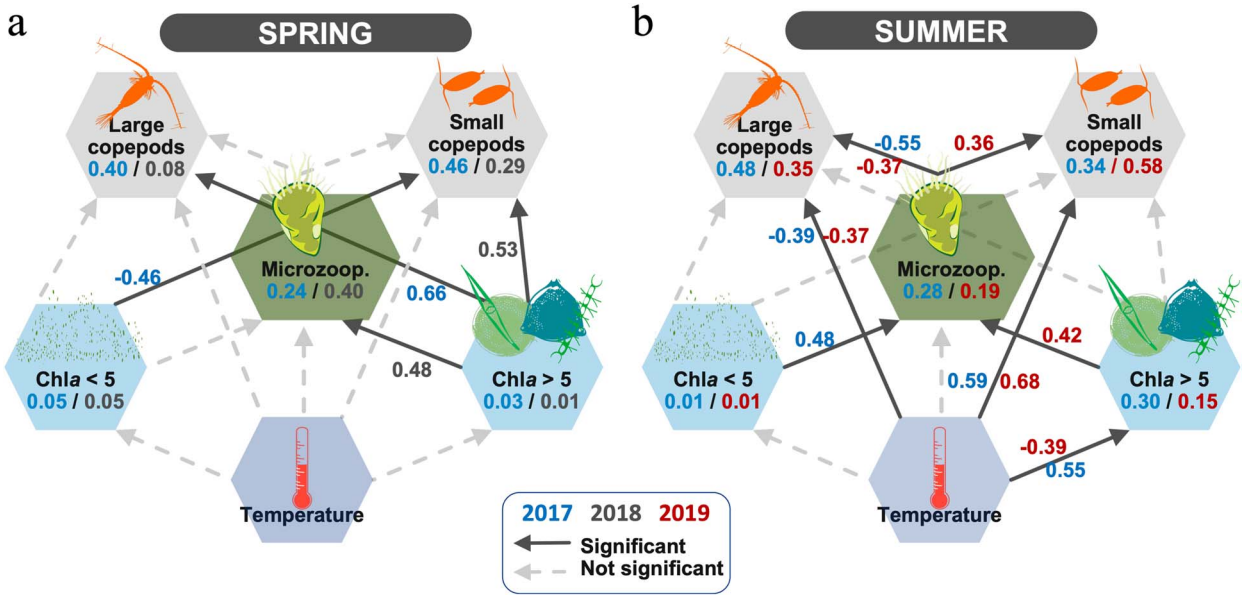

Fig. 7. Structural equation model path diagram for the spring (**a**) and summer (**b**) Arctic IERP surveys. The relative strength of associations is indicated by the standardized path coefficients. The values inside the box for each variable list the R^2_{adj}, representing the proportion of explained variance for that variable. Coefficients corresponding to 2017 are shown in blue, 2018 in gray, and 2019 in red. Tested, non-significant paths are shown in dashed light gray arrows. Water column mean temperature (°C), integrated concentrations of Chl*a* <5 μm and >5 μm (mg m^{-2}), integrated heterotrophic microzooplankton biomass (mg C m^{-2}), and total large and small copepod biomass (mg C m^{-2}) were included in the models.

Characterization of planktonic communities during summer

Summer of 2019 follows a series of years that started in 2014 with below average sea ice cover and high heat content in the Northern Bering and Chukchi seas that has been associated with enhanced southerly winds and elevated surface air temperatures (Danielson *et al.*, 2020). Unprecedented high temperatures and record low sea ice extent combined with a westward advection of the Alaskan Coastal Water (Danielson *et al.*, 2017) in 2019, caused the occurrence of shallow mixed layer depths throughout the Chukchi Sea (Jiao *et al.*, 2022). These conditions were associated with greater proportions of small-sized phytoplankton, particularly in areas with wCW. These areas dominated by small phytoplankton cells were associated with unusually high biomass of the small photosynthetic picocyanobacteria *Synechococcus* during summer 2019 (Lomas *et al.* in prep.). These results are consistent with reported trends of increasing proportions of the picophytoplankton size class with warmer ocean conditions (Morán *et al.*, 2010) and increasing biomass of *Synechococcus* during periods of high coastal water inflow (Paerl *et al.*, 2020). Also, the interaction between warming and decreased salinities that were observed broadly in summer of 2019 is known to reduce the contribution of large chain-forming diatoms (Sugie *et al.*, 2020). Summer of 2019 was also characterized by the occurrence of lower total microzooplankton biomass as a result of lower ciliates biomass. The predominance of small phytoplankton associated with warmer conditions would indicate more food available for microzooplankton. However, *Synechococcus*, an important component of the picophytoplankton in summer 2019 (Lomas *et al.* in prep.), constitutes a poor food source for ciliates and other microzooplankton compared to picoeukaryotes and nanophytoplankton and could explain low microzooplankton growth rates and observed low biomass in the region (Caron *et al.*, 1991; Jónasdóttir, 2019; Corradino and Schnetzer, 2022).

Warmer conditions in 2019 compared to 2017 were associated with increasing abundances of small copepods and of the neritic copepod species *T. discaudatus* and *E. longipedata*. Small copepods including *Oithona* spp., *Pseudocalanus* spp. and *Acartia longiremis*, and the larger neritic copepods *Centropages abdominalis*, *E. longipedata*, *T. discaudatus* are typically associated with Alaskan Coastal Water (Ershova *et al.*, 2015a; Pinchuk and Eisner, 2017), which was widespread during summer 2019. Kimmel *et al.* (2023) also reported the increases of these neritic species in warm years and attributed it to a westward expansion of Alaskan Coastal Water across both shelves during warm periods. The expansion of Coastal Water is linked to warmer conditions, as the coastal current transports warm water onto the shelf (Eisner *et al.*, 2020). In this way, Alaskan Coastal Water does not only carry smaller neritic species out over the shelf, but it also promotes the spread of smaller plankton species over larger ones, as warmer waters favor smaller species through faster population turnover, in the absence of food limitations (Kimmel *et al.*, 2023).

To further contextualize these warm-year observations, we examined copepod abundance data from two surveys conducted in summer 2012 and 2013, which were characterized as cold years (Kimmel *et al.*, 2023), using data from Pinchuk and Eisner (2017). Our comparison indicates that large *Calanus* spp. were, on average, approximately eight times more abundant in cold years (2012–2013) compared to warm years (2017–2019), while small *Pseudocalanus* spp. exhibited about eight times

greater abundance in warm years than in cold years. These findings are consistent with the broader pattern described by Kimmel *et al.* (2023), who reported an overall increase in small copepod abundance and a decrease in large copepod abundance during warm periods (2002–2005 and 2014–2018) compared to the cold period (2006–2013) in the Northern Bering Sea.

Planktonic interactions: correlative structure and implications on food web structure and efficiency

Seasonal differences in species and size composition of planktonic communities were reflected in the correlative structure of the planktonic food webs that may be indicative of seasonal differences in trophic web structure and efficiency. In spring, we observed higher Chl*a* concentrations dominated by large-sized phytoplankton (diatoms), whereas in late summer Chl*a* concentrations were low and predominantly composed of small-sized phytoplankton. In spring, as sea ice retreats, massive blooms of large-sized phytoplankton occur (Fujiwara *et al.*, 2016) favored by optimal light, nutrients and stratification. In summer in the Bering and Chukchi seas, stratification of the water column is strong and surface waters are typically nutrient-depleted resulting in a predominance of smaller sized phytoplankton in the surface (Eisner *et al.*, 2016; Giesbrecht *et al.*, 2019), including prasinophytes, haptophytes, and small dinoflagellates (Fujiwara *et al.*, 2014), with greater biomass of larger phytoplankton often present below the mixed layer (Martini *et al.*, 2016). Our observations of seasonal shifts in total Chl*a* concentrations, predominance of Chl*a* in the large-sized fraction, and diatom biomass are also consistent with phytoplankton taxonomic analysis from the Northern Bering and Chukchi seas (Sukhanova *et al.*, 2009; Laney and Sosik, 2014; Pickart *et al.*, 2019) and from seston fatty acid biomarker samples and FlowCAM images from the four Arctic IERP surveys (Nielsen *et al.*, 2023). These studies show community shifts from diatoms dominating in spring to higher predominance of dinoflagellates and small flagellates in summer. Decreasing diatom abundances and reduced nutritional quality under lower nutrient conditions are associated with decreases in high quality fatty acids towards late summer (Leu *et al.*, 2011; Nielsen *et al.*, 2023). These seasonal changes in phytoplankton biomass, composition and size structure, therefore, affect the quantity and quality of available food for microzooplankton and larger mesozooplankton (Søreide *et al.*, 2010; Leu *et al.*, 2011; Krause *et al.*, 2021). In our study, relatively high diatom and low microzooplankton biomass in spring were observed, along with a planktonic food web characterized by direct links between phytoplankton and copepod biomass with no significant links between copepod biomass and microzooplankton. In spring, microzooplankton growth rates are lower than diatoms due to low availability of phytoplankton prey (Sherr *et al.*, 2013) and low sea water temperatures. Additionally, microzooplankton biomass may be controlled by mesozooplankton consumption in the spring. As a result of the temporal lag between phytoplankton and microzooplankton biomass accumulation and potential top-down control of microzooplankton by mesozooplankton, diatom productivity largely escapes microzooplankton grazing losses, with only 23%–35% of diatoms grazed in spring bloom conditions (Krause *et al.*, 2021). Consequently, more diatom organic matter is directly available for secondary producers (e.g. copepods) and/or export to the benthos in spring. Indeed, while regional copepod species appear to prefer microzooplankton as prey (Campbell *et al.*, 2009), diatoms are the main diet of large mesozooplankton during spring due to the high disparity between diatom and microzooplankton biomass near the ice edge (Campbell *et al.*, 2009, 2016). These observations explain the strong association between large phytoplankton and large copepod biomass in spring of 2017. In spring of 2018, shifts in the timing of sea ice retreat and the spring bloom combined with very low abundances of large mesozooplankton may have weakened the strength of this association.

In summer, a greater predominance of smaller phytoplankton combined with high microzooplankton biomass was observed, along with associations between phytoplankton and large mesozooplankton fully mediated by microzooplankton (i.e. no direct effect of phytoplankton on large mesozooplankton). In summer, microzooplankton biomass and grazing pressure on diatoms are higher with a high proportion of diatoms (50%–100%) lost to microzooplankton grazing (Olson and Strom, 2002; Strom and Fredrickson, 2008; Yang *et al.*, 2015). At this time, microzooplankton carbon has been observed to exceed phytoplankton carbon (Olson and Strom, 2002; Strom and Fredrickson, 2008; Mitra *et al.*, 2014; Yang *et al.*, 2015). High microzooplankton biomass combined with the decline of diatom quality during post-bloom conditions result in microzooplankton dominating mesozooplankton diets during summer/autumn (Campbell *et al.*, 2009). Therefore, seasonal differences in plankton size structure and composition result in food webs with contrasting correlation structure although this structure is also dependent on oceanographic conditions that year (e.g. timing of sea ice retreat and water mass distributions). Overall, our results suggest that diatom production is funneled to mesozooplankton through microzooplankton in summer, which results in a less efficient trophic transfer of phytoplankton organic matter compared to spring (Sherr *et al.*, 2013; Stoecker *et al.*, 2014; Yang *et al.*, 2015; Krause *et al.*, 2021). Beyond these seasonal shifts in community interactions, the greater predominance of small zooplankton in our study period compared to colder years in summer (Pinchuk and Eisner, 2017; Kimmel *et al.*, 2023), likely reflects changes in phytoplankton size/quality between warm and cold years. This suggests that more complex trophic interactions may occur in the summer during warm years. As a result of warming and sea ice loss, Arctic systems are likely to have increasingly longer periods of time where this phytoplankton–microzooplankton–mesozooplankton food web is dominant as a result of warming and sea ice loss.

Perspectives: in the context of our findings, what might we expect in the future?

Changes in planktonic species composition and size structure have the potential to affect arctic marine ecosystems and the services they provide to human communities. Increases in primary production have been documented for the Northern Bering and Chukchi seas (Lewis *et al.*, 2020). However, it is uncertain if increased primary production will result in enhanced ecosystem productivity. Our findings suggest that a transition from a system fueled by ice-edge production to one dominated by open-water phytoplankton production would result in a less efficient trophic

food web (i.e. greater number of trophic links in food web) and therefore, less energy available for upper trophic levels (Lovvorn *et al.*, 2016). Decreases in ice algae and increases in open-water phytoplankton production due to sea ice loss or changes in the timing of sea ice retreat in spring, are correlated to shifts in the species and size composition of mesozooplankton communities, with a shift from large-bodied and typically lipid-rich zooplankton to smaller and often less nutritious zooplankton species (Siddon *et al.*, 2013; Aarflot *et al.*, 2018; Gorokhova, 2019; Møller and Nielsen, 2019; Hunt *et al.*, 2022). The decreases in biomass of large, typically high-lipid copepods with increases in temperature that we observed in all four surveys agree with observations from other studies conducted in the Bering and Chukchi seas (Spear *et al.*, 2020; Kimmel *et al.*, 2023). Changes in zooplankton prey quality may impact adult fish that are increasingly shifting their distributions northwards during low ice events (Stevenson and Lauth, 2019; Eisner *et al.*, 2020) as well as juvenile fish that rely on zooplankton prey for lipid acquisition prior to overwintering (Heintz *et al.*, 2013; Eisner *et al.*, 2020). Changes in plankton size structure also impact the amount of carbon input to the seafloor, as suggested by a strong positive relationship between benthic macrofaunal biomass and the proportion of large phytoplankton in the water column during the post-bloom period (Waga *et al.*, 2019) in the Bering and Chukchi seas. The effect of phytoplankton community size structure on benthic macrofauna can potentially impact upper trophic levels, such as marine mammals and diving seabirds in the Pacific Arctic (Grebmeier *et al.*, 2006; Waga *et al.*, 2020). A higher retention of pelagic production in the water column and decreased export to the benthos will weaken the tight benthic-pelagic coupling that is characteristic of the region (Grebmeier *et al.*, 1988). Other changes in species composition include the occurrence of harmful algal blooms (*Alexandrium* spp.) that have been documented in the Bering and Chukchi seas more frequently in association with increased northward advection of warm Pacific waters (Natsuike *et al.*, 2013; Natsuike *et al.*, 2017a, 2017b; Anderson *et al.*, 2021, 2023). The northern expansion of harmful algal blooms poses increasing threats to upper trophic levels and human health in the Arctic region (Anderson *et al.*, 2018; Huntington *et al.*, 2020). Our study shows that warming and increasing inflow of warm Coastal Water into the Chukchi Sea is associated with smaller sized phytoplankton (e.g. *Synechococcus*), and a mesozooplankton community characterized by small and neritic copepods in summer. Even though satellite models project increasing primary production for this region (Lewis *et al.*, 2020), the fate of that production and its ecosystem wide implications remain uncertain. A better understanding of the impacts of changes in planktonic species and size composition on higher trophic levels is critical and must be adequately accounted for in forecasting ecosystem responses to climate change.

Caveats and future directions

This study provides a synthesis of planktonic interactions based on correlative associations, but the lack of direct rate measurements limits mechanistic conclusions. Trophic interactions are influenced by factors such as prey selectivity, prey quality and temporal variability in prey availability. Future studies incorporating inverse carbon flow modeling approaches or targeted grazing measurements could help refine our understanding of planktonic trophic interactions in Arctic ecosystems.

Additionally, spatial differences in sampling coverage between years present a limitation, though our analyses suggest that seasonal shifts are the primary driver of plankton variability. The strong seasonal separation observed in community clustering and RDA results, even in regions with spatial overlaps, supports this interpretation. However, broader spatial sampling across both seasons would improve our ability to disentangle spatial and seasonal influences.

CONCLUSIONS

This study provides a comprehensive analysis of the variability in the distribution, size, and taxonomic compositions of phytoplankton, microzooplankton and mesozooplankton in the Northern Bering and Chukchi seas during the unusually warm period of 2017–2019. Our findings reveal significant shifts in plankton composition and interactions associated with changes in temperature, salinity, and nutrient availability. Record low sea ice in 2018 was associated with high biomass of large phytoplankton but low abundances of large mesozooplankton species in spring. In contrast, warm summer conditions and increased inflow of warm Coastal Water onto the Chukchi Sea shelf in 2019 resulted in a predominance of small-sized phytoplankton, reduced microzooplankton biomass, and a distinct mesozooplankton community characterized by high abundance and biomass of small pelagic and neritic copepod species. Seasonal differences in plankton species and size composition were reflected in the structure of planktonic food webs. In spring, there was a direct link between large phytoplankton and mesozooplankton, whereas in summer, the link was mediated by microzooplankton, indicating a more complex and less efficient trophic energy transfer. Our results suggest that a transition from ice-edge to open-water phytoplankton production with continued warming may lead to a less efficient trophic food web and reduced energy transfer to higher trophic levels. This shift, coupled with changes in zooplankton species composition towards smaller, less nutritious species, could impact on the overall productivity of the ecosystem and the species that rely on these food webs, including fish, marine mammals and seabirds.

ACKNOWLEDGEMENTS

The authors thank the captains and crews of the RV *Sikuliaq*, and RV *Ocean Starr* and the numerous scientists that participated in the surveys. Seth L. Danielson, Calvin W. Mordy, and Ryan McCabe are thanked for their assistance with nutrient and CTD data. We thank the Plankton Sorting and Identification Center in Szczecin, Poland. Gulce Kurtay and Matthieu Veron are thanked for their valuable comments on earlier drafts of the manuscript. We also thank the two anonymous reviewers whose suggestions significantly improved the paper. This research was part of SG National Research Council (NRC) postdoctoral fellowship at the National Oceanic and Atmospheric Administration (NOAA). Reference to trade names does not imply endorsement by the National Marine Fisheries Service, NOAA.

FUNDING

This research developed as part of the North Pacific Research Board (NPRB) Arctic Integrated Ecosystem Research Program (https://www.nprb.org/arctic-program; Baker *et al.*, 2023; this is NPRB publication no. ArcticIERP-55). S.G. was funded by NPRB through an NRC postdoctoral fellowship. J.M.N. is partially funded by the Cooperative Institute for Climate, Ocean, & Ecosystem Studies (CIOCES) under NOAA Cooperative Agreement (NA20OAR4320271). This is CICOES contribution 2024–1399 and EcoFOCI contribution EcoFOCI-1063.

DATA AVAILABILITY

Data used in our study are publicly available in the DataONE repository (https://arctic-ierp.dataportal.nprb.org/).

SUPPLEMENTARY DATA

Supplementary Data can be found at *Journal of Plankton Research* online.

REFERENCES

Aagaard, K., Weingartner, T. J., Danielson, S. L., Woodgate, R. A., Johnson, G. C. and Whitledge, T. E. (2006) Some controls on flow and salinity in Bering Strait. *Geophys. Res. Lett.*, **33**, 1–5.

Aarflot, J. M., Skjoldal, H. R., Dalpadado, P. and Skern-Mauritzen, M. (2018) Contribution of *Calanus* species to the mesozooplankton biomass in the Barents Sea. *ICES J. Mar. Sci.*, **75**, 2342–2354. https://doi.org/10.1093/icesjms/fsx221.

Akima, H. and Gebhardt, A. (2022) *Akima: Interpolation of Irregularly and Regularly Spaced Data*. R package version 0.6-3.4. The R Foundation for Statistical Computing. https://CRAN.R-project.org/package=akima.

Anderson, D. M., Fachon, E., Pickart, R. S., Lin, P., Fischer, A. D., Richlen, M. L., Uva, V., Brosnahan, M. L. *et al.* (2021) Evidence for massive and recurrent toxic blooms of *Alexandrium catenella* in the Alaskan Arctic. *Proc. Natl. Acad. Sci. USA*, **118**, e2107387118. https://doi.org/10.1073/pnas.2107387118.

Anderson, D. M., Richlen, M. L. and Lefebvre, K. A. (2018) Harmful algal blooms in the Arctic. In Osborne, E., Richter-Menge, J. and Jeffries, M. (eds.), *Arctic Report Card 2018*. U.S. National Oceanic and Atmospheric Administration, pp. 81–87.

Anderson, M. A., Fisk, A. T., Laing, R., Noël, M., Angnatok, J., Kirk, J., Evans, M., Pijogge, L. *et al.* (2023) Changing environmental conditions have altered the feeding ecology of two keystone Arctic marine predators. *Sci. Rep.*, **13**, 1–15.

Arrigo, K. R., Perovich, D. K., Pickart, R. S., Brown, Z. W., Van Dijken, G. L., Lowry, K. E., Mills, M. M., Palmer, M. A. *et al.* (2012) Massive phytoplankton blooms under Arctic Sea ice. *Science (1979)*, **336**, 1408. https://doi.org/10.1126/science.1215065.

Arrigo, K. R., Perovich, D. K., Pickart, R. S., Brown, Z. W., van Dijken, G. L., Lowry, K. E., Mills, M. M., Palmer, M. A. *et al.* (2014) Phytoplankton blooms beneath the sea ice in the Chukchi Sea. *Deep-Sea Res. II Top. Stud. Oceanogr.*, **105**, 1–16. https://doi.org/10.1016/j.dsr2.2014.03.018.

Axler, K. E., Goldstein, E. D., Nielsen, J. M., Deary, A. L. and Duffy-Anderson, J. T. (2023) Shifts in the composition and distribution of Pacific Arctic larval fish assemblages in response to rapid ecosystem change. *Glob. Chang. Biol.*, **29**, 4212–4233. https://doi.org/10.1111/gcb.16721.

Baker, M. R., Farley, E. V., Danielson, S. L., Mordy, C., Stafford, K. M. and Dickson, D. M. S. (2023) Integrated research in the Arctic—ecosystem linkages and shifts in the northern Bering Sea and eastern and western Chukchi Sea. *Deep-Sea Res. II Top. Stud. Oceanogr.*, **208**, 105251. https://doi.org/10.1016/j.dsr2.2023.105251.

Baker, M. R., Farley, E. V., Ladd, C., Danielson, S. L., Stafford, K. M., Huntington, H. P. and Dickson, D. M. S. (2020a) Integrated ecosystem research in the Pacific Arctic—understanding ecosystem processes, timing and change. *Deep-Sea Res. II Top. Stud. Oceanogr.*, **177**, 104850. https://doi.org/10.1016/j.dsr2.2020.104850.

Baker, M. R., Kivva, K. K., Pisareva, M. N., Watson, J. T. and Selivanova, J. (2020b) Shifts in the physical environment in the Pacific Arctic and implications for ecological timing and conditions. *Deep-Sea Res. II Top. Stud. Oceanogr.*, **177**, 104802. https://doi.org/10.1016/j.dsr2.2020.104802.

Ballinger, T. J. and Overland, J. E. (2022) The Alaskan Arctic regime shift since 2017: a harbinger of years to come? *Pol. Sci.*, **32**, 100841. https://doi.org/10.1016/j.polar.2022.100841.

Barnes, C., Maxwell, D., Reuman, D. C. and Jennings, S. (2010) Global patterns in predator-prey size relationships reveal size dependency of trophic transfer efficiency. *Ecology*, **91**, 222–232. https://doi.org/10.1890/08-2061.1.

Bocard, D., Gillet, F. and Legendre, P. (2011) *Numerical Ecology with R*, Springer, New York. https://doi.org/10.1007/978-1-4419-7976-6.

Boltovskoy, D. (1999) In Boltovskoy, D. (ed.), *South Atlantic Zooplankton*, Backhuys Publishers, Leiden.

Bray, J. R. and Curtis, J. T. (1957) An ordination of the upland forest communities of southern Wisconsin. *Ecol. Monogr.*, **27**, 325–349. https://doi.org/10.2307/1942268.

Campbell, R. G., Ashjian, C. J., Sherr, E. B., Sherr, B. F., Lomas, M. W., Ross, C., Alatalo, P., Gelfman, C. *et al.* (2016) Mesozooplankton grazing during spring sea-ice conditions in the eastern Bering Sea. *Deep-Sea Res. II Top. Stud. Oceanogr.*, **134**, 157–172. https://doi.org/10.1016/j.dsr2.2015.11.003.

Campbell, R. G., Sherr, E. B., Ashjian, C. J., Plourde, S., Sherr, B. F., Hill, V. and Stockwell, D. A. (2009) Mesozooplankton prey preference and grazing impact in the western Arctic Ocean. *Deep-Sea Res. II Top. Stud. Oceanogr.*, **56**, 1274–1289. https://doi.org/10.1016/j.dsr2.2008.10.027.

Caron, D. A., Countway, P. D., Jones, A. C. *et al.* (2012) Marine protistan diversity. *Annu. Rev. Mar. Sci.*, **4**, 467–493. https://doi.org/10.1146/annurev-marine-120709-142802.

Caron, D. A., Lim, E. L., Miceli, G., Waterbury, J. B. and Valois, F. W. (1991) Grazing and utilization of chroococcoid cyanobacteria and heterotrophic bacteria by protozoa in laboratory cultures and a coastal plankton community. *Mar. Ecol. Prog. Ser.*, **76**, 205–217. https://doi.org/10.3354/meps076205.

Carozza, D. A., Bianchi, D. and Galbraith, E. D. (2019) Metabolic impacts of climate change on marine ecosystems: implications for fish communities and fisheries. *Glob. Ecol. Biogeogr.*, **28**, 158–169. https://doi.org/10.1111/geb.12832.

Coello-Camba, A., Agustí, S., Vaqué, D., Holding, J., Arrieta, J. M., Wassmann, P. and Duarte, C. M. (2015) Experimental assessment of temperature thresholds for Arctic phytoplankton communities. *Estuar. Coasts*, **38**, 873–885. https://doi.org/10.1007/s12237-014-9849-7.

Corradino, G. L. and Schnetzer, A. (2022) Grazing of a heterotrophic nanoflagellate on prokaryote and eukaryote prey: ingestion rates and gross growth efficiency. *Mar. Ecol. Prog. Ser.*, **682**, 65–77. https://doi.org/10.3354/meps13921.

Danielson, S., Eisner, L., Weingartner, T. and Aagaard, K. (2011) Thermal and haline variability over the central Bering Sea shelf: seasonal and interannual perspectives. *Cont. Shelf Res.*, **31**, 539–554. https://doi.org/10.1016/j.csr.2010.12.010.

Danielson, S. L., Ahkinga, O., Ashjian, C., Basyuk, E., Cooper, L. W., Eisner, L., Farley, E., Iken, K. B. *et al.* (2020) Manifestation and consequences of warming and altered heat fluxes over the Bering and Chukchi Sea continental shelves. *Deep-Sea Res. II Top. Stud. Oceanogr.*, **177**, 104781. https://doi.org/10.1016/j.dsr2.2020.104781.

Danielson, S. L., Eisner, L., Ladd, C., Mordy, C., Sousa, L. and Weingartner, T. J. (2017) A comparison between late summer 2012 and 2013 water masses, macronutrients, and phytoplankton standing crops in the northern Bering and Chukchi seas. *Deep-Sea Res. II Top. Stud. Oceanogr.*, **135**, 7–26. https://doi.org/10.1016/j.dsr2.2016.05.024.

Danielson, S. L., Weingartner, T. J., Hedstrom, K. S., Aagaard, K., Woodgate, R., Curchitser, E. and Stabeno, P. J. (2014) Coupled wind-forced controls of the Bering-Chukchi shelf circulation and the Bering Strait throughflow: Ekman transport, continental shelf waves, and variations of the Pacific-Arctic Sea surface height gradient. *Prog. Oceanogr.*, **125**, 40–61. https://doi.org/10.1016/j.pocean.2014.04.006.

Daufresne, M., Lengfellner, K. and Sommer, U. (2009) Global warming benefits the small in aquatic ecosystems. *Proc. Natl. Acad. Sci. USA*, **106**, 12788–12793. https://doi.org/10.1073/pnas.0902080106.

De Cáceres, M. and Legendre, P. (2009) Associations between species and groups of sites: indices and statistical inference. *Ecology*, **90**, 3566–3574. https://doi.org/10.1890/08-1823.1.

Dufrêne, M. and Legendre, P. (1997) Species assemblages and indicator species: the need for a flexible asymmetrical approach. *Ecol. Monogr.*, **67**, 345–366. https://doi.org/10.2307/2963459.

Eisner, L. B., Gann, J. C., Ladd, C. D., Cieciel, K. and Mordy, C. W. (2016) Late summer/early fall phytoplankton biomass (chlorophyll a) in the eastern Bering Sea: spatial and temporal variations and factors affecting chlorophyll a concentrations. *Deep-Sea Res. II Top. Stud. Oceanogr.*, **134**, 100–114. https://doi.org/10.1016/j.dsr2.2015.07.012.

Eisner, L. B., Zuenko, Y. I., Basyuk, E. O., Britt, L. L., Duffy-Anderson, J. T., Kotwicki, S., Ladd, C. and Cheng, W. (2020) Environmental impacts on walleye Pollock (*Gadus chalcogrammus*) distribution across the Bering Sea shelf. *Deep-Sea Res. II Top. Stud. Oceanogr.*, **181-182**, 104881. https://doi.org/10.1016/j.dsr2.2020.104881.

Ershova, E. A., Hopcroft, R. R. and Kosobokova, K. N. (2015a) Inter-annual variability of summer mesozooplankton communities of the western Chukchi Sea: 2004–2012. *Polar Biol.*, **38**, 1461–1481. https://doi.org/10.1007/s00300-015-1709-9.

Ershova, E. A., Hopcroft, R. R., Kosobokova, K. N., Matsuno, K., Nelson, R. J., Yamaguchi, A. and Eisner, L. B. (2015b) Long-term changes in summer zooplankton communities of the Western Chukchi Sea, 1945–2012. *Oceanography*, **28**, 100–115. https://doi.org/10.5670/oceanog.2015.60.

Franzè, G. and Lavrentyev, P. J. (2014) Microzooplankton growth rates examined across a temperature gradient in the Barents Sea. *PLoS One*, **9**, e86429. https://doi.org/10.1371/journal.pone.0086429.

Fujiwara, A., Hirawake, T., Suzuki, K., Eisner, L., Imai, I., Nishino, S., Kikuchi, T. and Saitoh, S. I. (2016) Influence of timing of sea ice retreat on phytoplankton size during marginal ice zone bloom period on the Chukchi and Bering shelves. *Biogeosciences*, **13**, 115–131. https://doi.org/10.5194/bg-13-115-2016.

Fujiwara, A., Hirawake, T., Suzuki, K., Imai, I. and Saitoh, S. I. (2014) Timing of sea ice retreat can alter phytoplankton community structure in the western Arctic Ocean. *Biogeosciences*, **11**, 1705–1716. https://doi.org/10.5194/bg-11-1705-2014.

Fujiwara, M. and Cohen, J. E. (2015) Mean and variance of population density and temporal Taylor's law in stochastic stage-structured density-dependent models of exploited fish populations. *Theor. Ecol.*, **8**, 175–186. https://doi.org/10.1007/s12080-014-0242-8.

Fulfer, V. M. and Menden-Deuer, S. (2021) Heterotrophic dinoflagellate growth and grazing rates reduced by microplastic ingestion. *Front. Mar. Sci.*, **8**, 716349. https://doi.org/10.3389/fmars.2021.716349.

Galloway, A. W. E. and Winder, M. (2015) Partitioning the relative importance of phylogeny and environmental conditions on phytoplankton fatty acids. *PLoS One*, **10**, 1–23. https://doi.org/10.1371/journal.pone.0130053.

García-Oliva, O., Hantzsche, F. M., Boersma, M. and Wirtz, K. W. (2022) Phytoplankton and particle size spectra indicate intense mixotrophic dinoflagellates grazing from summer to winter. *J. Plankton Res.*, **44**, 224–240. https://doi.org/10.1093/plankt/fbac013.

Gardner, J. L., Peters, A., Kearney, M. R., Joseph, L. and Heinsohn, R. (2011) Declining body size: a third universal response to warming? *Trends Ecol. Evol.*, **26**, 285–291. https://doi.org/10.1016/j.tree.2011.03.005.

Gawarkiewicz, G., Haney, J. C. and Caruso, M. J. (1994) Summertime synoptic variability of frontal systems in the northern Bering Sea. *J. Geophys. Res. Oceans*, **99**, 7617–7625. https://doi.org/10.1029/94JC00259.

Giesbrecht, K. E., Varela, D. E., Wiktor, J., Grebmeier, J. M., Kelly, B. and Long, J. E. (2019) A decade of summertime measurements of phytoplankton biomass, productivity and assemblage composition in the Pacific Arctic region from 2006 to 2016. *Deep-Sea Res. II Top. Stud. Oceanogr.*, **162**, 93–113. https://doi.org/10.1016/j.dsr2.2018.06.010.

Gordon, L. L., Jennings, J. C. Jr., Ross, A. A. and Krest, J. M. (1993) A suggested protocol for continuous flow automated analysis of seawater nutrients (phosphate, nitrate, nitrite and silicic acid) in the WOCE Hydrographic Program and the Joint Global Ocean Fluxes Study. In *WOCE Hydrographic Program Office, Methods Manual*. Woods Hole, MA: WOCE Hydrographic Programme Office, pp. 1–52.

Gorokhova, E. (2019) Individual body size as a predictor of lipid storage in Baltic Sea zooplankton. *J. Plankton Res.*, **41**, 273–280. https://doi.org/10.1093/plankt/fbz010.

Grace, J. B., Anderson, T. M., Olff, H. and Scheiner, S. (2010) On the specification of structural equation models for ecological systems. *Ecol. Monogr.*, **80**, 67–87. https://doi.org/10.1890/09-0464.1.

Grace, J. B. and Keeley, J. E. (2006) A structural equation model analysis of postfire plant diversity in California shrublands. *Ecol. Appl.*, **16**, 503–514. https://doi.org/10.1890/1051-0761(2006)016[0503:ASEMAO]2.0.CO;2.

Grebmeier, J., McRoy, C. and Feder, H. (1988) Pelagic-benthic coupling on the shelf of the northern Bering and Chukchi seas. I. Food supply source and benthic biomass. *Mar. Ecol. Prog. Ser.*, **48**, 57–67. https://doi.org/10.3354/meps048057.

Grebmeier, J. M. (2012) Shifting patterns of life in the Pacific Arctic and sub-Arctic seas. *Annu. Rev. Mar. Sci.*, **4**, 63–78. https://doi.org/10.1146/annurev-marine-120710-100926.

Grebmeier, J. M., Bluhm, B. A., Cooper, L. W., Denisenko, S. G., Iken, K., Kędra, M. and Serratos, C. (2015) Time-series benthic community composition and biomass and associated environmental characteristics in the Chukchi Sea during the RUSALCA 2004–2012 program. *Oceanography*, **28**, 116–133. https://doi.org/10.5670/oceanog.2015.61.

Grebmeier, J. M., Overland, J. E., Moore, S. E., Farley, E. V., Carmack, E. C., Cooper, L. W., Frey, K. E., Helle, J. H. *et al.* (2006) A major ecosystem shift in the northern Bering Sea. *Science (1979)*, **311**, 1461–1464. https://doi.org/10.1126/science.1121365.

Hansen, B., Bjornsen, P. K. and Hansen, P. J. (1994) The size ratio between planktonic predators and their prey. *Limnol. Oceanogr.*, **39**, 395–403. https://doi.org/10.4319/lo.1994.39.2.0395.

Hansen, P. J., Bjørnsen, P. K. and Hansen, B. W. (1997) Zooplankton grazing and growth: scaling within the 2-2,-μm body size range. *Limnol. Oceanogr.*, **42**, 687–704. https://doi.org/10.4319/lo.1997.42.4.0687.

Heintz, R. A., Siddon, E. C., Farley, E. V. and Napp, J. M. (2013) Correlation between recruitment and fall condition of age-0 Pollock (*Theragra chalcogramma*) from the eastern Bering Sea under varying climate conditions. *Deep-Sea Res. II Top. Stud. Oceanogr.*, **94**, 150–156. https://doi.org/10.1016/j.dsr2.2013.04.006.

Hill, V. J., Light, B., Steele, M. and Zimmerman, R. C. (2018) Light availability and phytoplankton growth beneath arctic sea ice: integrating observations and modeling. *J. Geophys. Res. Oceans*, **123**, 3651–3667. https://doi.org/10.1029/2017JC013617.

Hirawake, T., Oida, J., Yamashita, Y., Waga, H., Abe, H., Nishioka, J., Nomura, D., Ueno, H. *et al.* (2021) Water mass distribution in the northern Bering and southern Chukchi seas using light absorption of chromophoric dissolved organic matter. *Prog. Oceanogr.*, **197**, 102641. https://doi.org/10.1016/j.pocean.2021.102641.

Hirst, A. G. and Bunker, A. J. (2003) Growth of marine planktonic copepods: Global rates and patterns in relation to chlorophyll a, temperature, and body weight. *Limnology & Oceanography*, **48**, 1988–2010. https://doi.org/10.4319/lo.2003.48.5.1988.

Holmes, R. M., Aminot, A., Kerouel, R., Hooker, B. A. and Peterson, B. J. (1999) A simple and precise method for measuring ammonium

in marine and freshwater ecosystems. *Can. J. Fish. Aquat. Sci.*, **56**, 1801–1808. https://doi.org/10.1139/f99-128.

Hunt, G. L., Blanchard, A. L., Boveng, P., Dalpadado, P., Drinkwater, K. F., Eisner, L., Hopcroft, R. R., Kovacs, K. M. *et al.* (2013) The Barents and Chukchi seas: comparison of two Arctic shelf ecosystems. *J. Mar. Syst.*, **109-110**, 43–68. https://doi.org/10.1016/j.jmarsys.2012.08.003.

Hunt, G. L., Drinkwater, K. F., Arrigo, K., Berge, J., Daly, K. L., Danielson, S., Daase, M., Hop, H. *et al.* (2016) Advection in polar and sub-polar environments: impacts on high latitude marine ecosystems. *Prog. Oceanogr.*, **149**, 40–81. https://doi.org/10.1016/j.pocean.2016.10.004.

Hunt, G. L., Yasumiishi, E. M., Eisner, L. B., Stabeno, P. J. and Decker, M. B. (2022) Climate warming and the loss of sea ice: the impact of sea-ice variability on the southeastern Bering Sea pelagic ecosystem. *ICES J. Mar. Sci.*, **79**, 937–953. https://doi.org/10.1093/icesjms/fsaa206.

Huntington, H. P., Danielson, S. L., Wiese, F. K., Baker, M., Boveng, P., Citta, J. J., De Robertis, A., Dickson, D. M. S. *et al.* (2020) Evidence suggests potential transformation of the Pacific Arctic ecosystem is underway. *Nat. Clim. Chang.*, **10**, 342–348.

Incze, L. S., Siefert, D. W. and Napp, J. M. (1997) Mesozooplankton of Shelikof Strait, Alaska: abundance and community composition. *Cont. Shelf Res.*, **17**, 287–305. https://doi.org/10.1016/S0278-4343(96)00036-2.

Irisson, J. (2024) *Castr: Process CTD Casts*. R package version 0.1.0. GitHub repository hosted at https://github.com/jiho/castr.

Jay, C. V., Fischbach, A. S. and Kochnev, A. A. (2012) Walrus areas of use in the Chukchi Sea during sparse sea ice cover. *Mar. Ecol. Prog. Ser.*, **468**, 1–13. https://doi.org/10.3354/meps10057.

Jiao, X., Zhang, J., Li, Q. and Li, C. (2022) Observational study on the variability of mixed layer depth in the Bering Sea and the Chukchi Sea in the summer of 2019. *Front. Mar. Sci.*, **9**, 1–13. https://doi.org/10.3389/fmars.2022.862857.

Jónasdóttir, S. H. (2019) Fatty acid profiles and production in marine phytoplankton. *Mar. Drugs*, **17**, 151. https://doi.org/10.3390/md17030151.

Kikuchi, G., Abe, H., Hirawake, T. and Sampei, M. (2020) Distinctive spring phytoplankton bloom in the Bering Strait in 2018: a year of historically minimum sea ice extent. *Deep-Sea Res. II Top. Stud. Oceanogr.*, **181-182**, 104905. https://doi.org/10.1016/j.dsr2.2020.104905.

Kimmel, D., Eisner, L. and Pinchuk, A. (2023) The northern Bering Sea zooplankton community response to variability in sea ice: evidence from a series of warm and cold periods. *Mar. Ecol. Prog. Ser.*, **705**, 21–42. https://doi.org/10.3354/meps14237.

Kimura, F., Abe, Y., Matsuno, K., Hopcroft, R. R. and Yamaguchi, A. (2020) Seasonal changes in the zooplankton community and population structure in the northern Bering Sea from June to September, 2017. *Deep-Sea Res. II Top. Stud. Oceanogr.*, **181-182**, 104901. https://doi.org/10.1016/j.dsr2.2020.104901.

Kimura, F., Matsuno, K., Abe, Y. and Yamaguchi, A. (2022) Effects of early sea-ice reduction on zooplankton and copepod population structure in the Northern Bering Sea during the summers of 2017 and 2018. *Front. Mar. Sci.*, **9**, 808910. https://doi.org/10.3389/fmars.2022.808910.

Krause, J. W., Lomas, M. W. and Danielson, S. L. (2021) Diatom growth, biogenic silica production, and grazing losses to microzooplankton during spring in the northern Bering and Chukchi seas. *Deep-Sea Res. II Top. Stud. Oceanogr.*, **191-192**, 104950. https://doi.org/10.1016/j.dsr2.2021.104950.

Kwok, R. (2018) Arctic Sea ice thickness, volume, and multiyear ice coverage: losses and coupled variability (1958-2018). *Environ. Res. Lett.*, **13**, 105005. https://doi.org/10.1088/1748-9326/aae3ec.

Kwon, S., Lee, I., Park, K., Cho, K. H., Jung, J., Park, T., Lee, Y., Jeon, C. *et al.* (2022) Summer net community production in the northern Chukchi Sea: comparison between 2017 and 2020. *Front. Mar. Sci.*, **9**, 1–15.

Laney, S. R. and Sosik, H. M. (2014) Phytoplankton assemblage structure in and around a massive under-ice bloom in the Chukchi Sea. *Deep-Sea Res. II Top. Stud. Oceanogr.*, **105**, 30–41. https://doi.org/10.1016/j.dsr2.2014.03.012.

Lefcheck, J. S. (2016) piecewiseSEM: piecewise structural equation modelling in r for ecology, evolution, and systematics. *Methods Ecol. Evol.*, **7**, 573–579. https://doi.org/10.1111/2041-210X.12512.

Leu, E., Søreide, J. E., Hessen, D. O., Falk-Petersen, S. and Berge, J. (2011) Consequences of changing sea-ice cover for primary and secondary producers in the European Arctic shelf seas: timing, quantity, and quality. *Prog. Oceanogr.*, **90**, 18–32. https://doi.org/10.1016/j.pocean.2011.02.004.

Lewis, K. L., van Dijken, G. L. and Arrigo, K. R. (2020) Changes in phytoplankton concentration, not sea ice, now drive increased Arctic Ocean primary production. *Science (1979)*, **202**, 198–202.

Li, W. K. W., McLaughlin, F. A., Lovejoy, C. and Carmack, E. C. (2009) Smallest algae thrive as the Arctic Ocean freshens. *Science (1979)*, **326**, 539. https://doi.org/10.1126/science.1179798.

Lovvorn, J. R., North, C. A., Kolts, J. M., Grebmeier, J. M., Cooper, L. W. and Cui, X. (2016) Projecting the effects of climate-driven changes in organic matter supply on benthic food webs in the northern Bering Sea. *Mar. Ecol. Prog. Ser.*, **548**, 11–30. https://doi.org/10.3354/meps11651.

Markus, T., Stroeve, J. C. and Miller, J. (2009) Recent changes in Arctic Sea ice melt onset, freezeup, and melt season length. *J. Geophys. Res. Oceans*, **114**, 1–14. https://doi.org/10.1029/2009JC005436.

Martini, K. I., Stabeno, P. J., Ladd, C., Winsor, P., Weingartner, T. J., Mordy, C. W. and Eisner, L. B. (2016) Dependence of subsurface chlorophyll on seasonal water masses in the Chukchi Sea. *J. Geophys. Res. Oceans*, **121**, 1755–1770. https://doi.org/10.1002/2015JC011359.

Menden-Deuer, S. and Lessard, E. J. (2000) Carbon to volume relationships for dinoflagellates, diatoms, and other protist plankton. *Limnol. Oceanogr.*, **45**, 569–579. https://doi.org/10.4319/lo.2000.45.3.0569.

Mitra, A., Caron, D. A., Faure, E., Flynn, K. J., Leles, S. G., Hansen, P. J., McManus, G. B., Not, F. *et al.* (2023) The Mixoplankton database (MDB): diversity of photo-phago-trophic plankton in form, function, and distribution across the global ocean. *J. Eukaryot. Microbiol.*, **70**, 1–25. https://doi.org/10.1111/jeu.12972.

Mitra, A., Flynn, K. J., Burkholder, J. M., Berge, T., Calbet, A., Raven, J. A., Granéli, E., Glibert, P. M. *et al.* (2014) The role of mixotrophic protists in the biological carbon pump. *Biogeosciences*, **11**, 995–1005. https://doi.org/10.5194/bg-11-995-2014.

Møller, E. F. and Nielsen, T. G. (2019) Borealization of Arctic zooplankton—smaller and less fat zooplankton species in Disko Bay, Western Greenland. *Limnol. Oceanogr.*, **65**, 1175–1188.

Morán, X. A. G., López-Urrutia, Á., Calvo-Díaz, A. and Li, W. K. W. (2010) Increasing importance of small phytoplankton in a warmer ocean. *Glob. Chang. Biol.*, **16**, 1137–1144. https://doi.org/10.1111/j.1365-2486.2009.01960.x.

Mueter, F. J., Planque, B., Hunt, G. L. Jr., Alabia, I. D., Hirawake, T., Eisner, L., Dalpadado, P., Drinkwater, K. F. *et al.* (2021) Possible future scenarios in the gateways to the Arctic for subarctic and Arctic marine systems: prey resources, food webs, fish, and fisheries. *ICES J. Mar. Sci.*, **78**, 3017–3045. https://doi.org/10.1093/icesjms/fsab122.

Mundy, C. J., Barber, D. G. and Michel, C. (2005) Variability of snow and ice thermal, physical and optical properties pertinent to sea ice algae biomass during spring. *J. Mar. Syst.*, **58**, 107–120. https://doi.org/10.1016/j.jmarsys.2005.07.003.

Napp, J. M., Incze, L. S., Ortner, P. B., Siefert, D. L. W. and Britt, L. (1996) The plankton of Shelikof Strait, Alaska: standing stock, production, mesoscale variability and their relevance to larval fish survival. *Fish. Oceanogr.*, **5**, 19–38. https://doi.org/10.1111/j.1365-2419.1996.tb00080.x.

Natsuike, M., Matsuno, K., Hirawake, T., Yamaguchi, A., Nishino, S. and Imai, I. (2017a) Possible spreading of toxic *Alexandrium tamarense* blooms on the Chukchi Sea shelf with the inflow of Pacific summer water due to climatic warming. *Harmful Algae*, **61**, 80–86. https://doi.org/10.1016/j.hal.2016.11.019.

Natsuike, M., Nagai, S., Matsuno, K., Saito, R., Tsukazaki, C., Yamaguchi, A. and Imai, I. (2013) Abundance and distribution of toxic

Alexandrium tamarense resting cysts in the sediments of the Chukchi Sea and the eastern Bering Sea. *Harmful Algae*, **27**, 52–59. https://doi.org/10.1016/j.hal.2013.04.006.

Natsuike, M., Saito, R., Fujiwara, A., Matsuno, K., Yamaguchi, A., Shiga, N., Hirawake, T., Kikuchi, T. *et al.* (2017b) Evidence of increased toxic *Alexandrium tamarense* dinoflagellate blooms in the eastern Bering Sea in the summers of 2004 and 2005. *PLoS One*, **12**, 1–13. https://doi.org/10.1371/journal.pone.0188565.

Nielsen, J. M., Copeman, L. A., Eisner, L. B., Axler, K. E., Mordy, C. W. and Lomas, M. W. (2023) Phytoplankton and seston fatty acid dynamics in the northern Bering-Chukchi Sea region. *Deep-Sea Res. II Top. Stud. Oceanogr.*, **208**, 105247. https://doi.org/10.1016/j.dsr2.2022.105247.

Nielsen, J. M., Sigler, M. F., Eisner, L. B., Watson, J. T., Rogers, L. A., Bell, S. W., Pelland, N., Mordy, C. W. *et al.* (2024) Spring phytoplankton bloom phenology during recent climate warming on the Bering Sea shelf. *Prog. Oceanogr.*, **220**, 103176. https://doi.org/10.1016/j.pocean.2023.103176.

Oksanen, J., Simpson, G., Blanchet, F., Kindt, R., Legendre, P., Minchin, P., O'Hara, R., Solymos, P. *et al.* (2022) *Vegan: Community Ecology Package*. R package version 2.6-4. The R Foundation for Statistical Computing. https://CRAN.R-project.org/package=vegan.

Olson, M. B. and Strom, S. L. (2002) Phytoplankton growth, microzooplankton herbivory and community structure in the southeast Bering Sea: insight into the formation and temporal persistence of an *Emiliania huxleyi* bloom. *Deep-Sea Res. II Top. Stud. Oceanogr.*, **49**, 5969–5990. https://doi.org/10.1016/S0967-0645(02)00329-6.

Paerl, R. W., Venezia, R. E., Sanchez, J. J. and Paerl, H. W. (2020) Picophytoplankton dynamics in a large temperate estuary and impacts of extreme storm events. *Sci. Rep.*, **10**, 1–15.

Park, J., Lee, S., Jo, Y. H. and Kim, H. C. (2021) Phytoplankton bloom changes under extreme geophysical conditions in the northern Bering Sea and the southern Chukchi Sea. *Remote Sens.*, **13**, 4035. https://doi.org/10.3390/rs13204035.

Parsons, T. R. (1984) *A Manual of Chemical & Biological Methods for Seawater Analysis*. Amsterdam: Elsevier.

Pickart, R. S., Nobre, C., Lin, P., Arrigo, K. R., Ashjian, C. J., Berchok, C., Cooper, L. W., Grebmeier, J. M. *et al.* (2019) Seasonal to mesoscale variability of water masses and atmospheric conditions in Barrow canyon, Chukchi Sea. *Deep-Sea Res. II Top. Stud. Oceanogr.*, **162**, 32–49. https://doi.org/10.1016/j.dsr2.2019.02.003.

Pinchuk, A. I. and Eisner, L. B. (2017) Spatial heterogeneity in zooplankton summer distribution in the eastern Chukchi Sea in 2012–2013 as a result of large-scale interactions of water masses. *Deep-Sea Res. II Top. Stud. Oceanogr.*, **135**, 27–39. https://doi.org/10.1016/j.dsr2.2016.11.003.

Questel, J. M., Clarke, C. and Hopcroft, R. R. (2013) Seasonal and interannual variation in the planktonic communities of the northeastern Chukchi Sea during the summer and early fall. *Cont. Shelf Res.*, **67**, 23–41. https://doi.org/10.1016/j.csr.2012.11.003.

Rosseel, Y. (2012) Lavaan: an R package for structural equation modeling. *J. Stat. Softw.*, **48**, 1–36.

Serreze, M. C., Crawford, A. D., Stroeve, J. C., Barrett, A. P. and Woodgate, R. A. (2016) Variability, trends, and predictability of seasonal sea ice retreat and advance in the Chukchi Sea. *J. Geophys. Res. Oceans*, **121**, 7308–7325. https://doi.org/10.1002/2016JC011977.

Sherr, E. B., Sherr, B. F. and Ross, C. (2013) Microzooplankton grazing impact in the Bering Sea during spring sea ice conditions. *Deep-Sea Res. II Top. Stud. Oceanogr.*, **94**, 57–67. https://doi.org/10.1016/j.dsr2.2013.03.019.

Siddon, E. C., Kristiansen, T., Mueter, F. J., Holsman, K. K., Heintz, R. A. and Farley, E. V. (2013) Spatial match-mismatch between juvenile fish and prey provides a mechanism for recruitment variability across contrasting climate conditions in the eastern Bering Sea. *PLoS One*, **8**, e84526. https://doi.org/10.1371/journal.pone.0084526.

Siddon, E. C., Zador, S. G. and Hunt, G. L. (2020) Ecological responses to climate perturbations and minimal sea ice in the northern Bering Sea. *Deep-Sea Res. II Top. Stud. Oceanogr.*, **181-182**, 104914. https://doi.org/10.1016/j.dsr2.2020.104914.

Song, H., Ji, R., Jin, M., Li, Y., Feng, Z., Varpe, Ø. and Davis, C. S. (2021) Strong and regionally distinct links between ice-retreat timing and phytoplankton production in the Arctic Ocean. *Limnol. Oceanogr.*, **66**, 2498–2508. https://doi.org/10.1002/lno.11768.

Søreide, J. E., Leu, E. V. A., Berge, J., Graeve, M. and Falk-Petersen, S. (2010) Timing of blooms, algal food quality and *Calanus glacialis* reproduction and growth in a changing Arctic. *Glob. Chang. Biol.*, **16**, 3154–3163. https://doi.org/10.1111/j.1365-2486.2010.02175.x.

Spear, A., Napp, J., Ferm, N. and Kimmel, D. (2020) Advection and in situ processes as drivers of change for the abundance of large zooplankton taxa in the Chukchi Sea. *Deep-Sea Res. II Top. Stud. Oceanogr.*, **177**, 104814. https://doi.org/10.1016/j.dsr2.2020.104814.

Springer, A. M., Peter McRoy, C. and Flint, M. V. (1996) The Bering Sea Green Belt: shelf-edge processes and ecosystem production. *Fish. Oceanogr.*, **5**, 205–223. https://doi.org/10.1111/j.1365-2419.1996.tb00118.x.

Stabeno, P. J., Bell, S. W., Bond, N. A., Kimmel, D. G., Mordy, C. W. and Sullivan, M. E. (2019) Distributed biological observatory region 1: physics, chemistry and plankton in the northern Bering Sea. *Deep-Sea Res. II Top. Stud. Oceanogr.*, **162**, 8–21. https://doi.org/10.1016/j.dsr2.2018.11.006.

Stevenson, D. E. and Lauth, R. R. (2019) Bottom trawl surveys in the northern Bering Sea indicate recent shifts in the distribution of marine species. *Polar Biol.*, **42**, 407–421. https://doi.org/10.1007/s00300-018-2431-1.

Stigebrandt, A. (1984) The North Pacific: a global-scale estuary. *J. Phys. Oceanogr.*, **14**, 464–470. https://doi.org/10.1175/1520-0485(1984)014<0464:TNPAGS>2.0.CO;2.

Stoecker, D. K., Hansen, P. J., Caron, D. A. and Mitra, A. (2017) Mixotrophy in the marine plankton. *Annu. Rev. Mar. Sci.*, **9**, 311–335. https://doi.org/10.1146/annurev-marine-010816-060617.

Stoecker, D. K., Weigel, A. and Goes, J. I. (2014) Microzooplankton grazing in the eastern Bering Sea in summer. *Deep-Sea Res. II Top. Stud. Oceanogr.*, **109**, 145–156. https://doi.org/10.1016/j.dsr2.2013.09.017.

Stroeve, J. and Notz, D. (2018) Changing state of Arctic Sea ice across all seasons. *Environ. Res. Lett.*, **13**, 103001. https://doi.org/10.1088/1748-9326/aade56.

Strom, S. L. and Fredrickson, K. A. (2008) Intense stratification leads to phytoplankton nutrient limitation and reduced microzooplankton grazing in the southeastern Bering Sea. *Deep-Sea Res. II Top. Stud. Oceanogr.*, **55**, 1761–1774. https://doi.org/10.1016/j.dsr2.2008.04.008.

Sugie, K., Fujiwara, A., Nishino, S., Kameyama, S. and Harada, N. (2020) Impacts of temperature, CO2, and salinity on phytoplankton community composition in the Western Arctic Ocean. *Front. Mar. Sci.*, **6**, 821. https://doi.org/10.3389/fmars.2019.00821.

Sukhanova, I. N., Flint, M. V., Pautova, L. A., Stockwell, D. A., Grebmeier, J. M. and Sergeeva, V. M. (2009) Phytoplankton of the western Arctic in the spring and summer of 2002: structure and seasonal changes. *Deep-Sea Res. II Top. Stud. Oceanogr.*, **56**, 1223–1236. https://doi.org/10.1016/j.dsr2.2008.12.030.

Timmermans, M. L. and Labe, Z. (2020) *Sea Surface Temperature*. Silver Spring, Maryland, USA: NOAA Arctic Report Card.

Tomas, C. R. (1997) *Identifying Marine Phytoplankton*. San Diego, California, USA: Academic Press.

Utermöhl, H. (1958) Zur Vervollkommnung der quantitativen phytoplankton-Methodik. *Mitteilungen der Internationalen Vereinigung der Limnologen*, **9**, 1–38. https://doi.org/10.1080/05384680.1958.11904091.

Waga, H. and Hirawake, T. (2020) Changing occurrences of fall blooms associated with variations in phytoplankton size structure in the Pacific Arctic. *Front. Mar. Sci.*, **7**, 1–12.

Waga, H., Hirawake, T., Fujiwara, A., Grebmeier, J. M. and Saitoh, S. I. (2019) Impact of spatiotemporal variability in phytoplankton size

structure on benthic macrofaunal distribution in the Pacific Arctic. *Deep-Sea Res. II Top. Stud. Oceanogr.*, **162**, 114–126. https://doi.org/10.1016/j.dsr2.2018.10.008.

Waga, H., Hirawake, T. and Grebmeier, J. M. (2020) Recent change in benthic macrofaunal community composition in relation to physical forcing in the Pacific Arctic. *Polar Biol.*, **43**, 285–294. https://doi.org/10.1007/s00300-020-02632-3.

Walsh, J. J. (1989) Arctic carbon sinks: present and future. *Glob. Biogeochem. Cycles*, **3**, 393–411. https://doi.org/10.1029/GB003i004p00393.

Weingartner, T., Aagaard, K., Woodgate, R., Danielson, S., Sasaki, Y. and Cavalieri, D. (2005) Circulation on the north Central Chukchi Sea shelf. *Deep-Sea Res. II Top. Stud. Oceanogr.*, **52**, 3150–3174. https://doi.org/10.1016/j.dsr2.2005.10.015.

Woodgate, R. A., Aagaard, K. and Weingartner, T. J. (2005) Monthly temperature, salinity, and transport variability of the Bering Strait through flow. *Geophys. Res. Lett.*, **32**, 1–4.

Wu, Z. and Wang, X. (2018) Variability of Arctic Sea ice (1979-2016). *Water (Basel)*, **11**, 1–10. https://doi.org/10.3390/w11010023.

Yang, E. J., Ha, H. K. and Kang, S. H. (2015) Microzooplankton community structure and grazing impact on major phytoplankton in the Chukchi Sea and the western Canada basin, Arctic Ocean. *Deep-Sea Res. II Top. Stud. Oceanogr.*, **120**, 91–102. https://doi.org/10.1016/j.dsr2.2014.05.020.

Journal of Plankton Research, 2025, Vol. 47, No. 4, fbaf034
https://doi.org/10.1093/plankt/fbaf034
Original Article